Ror2-mediated non-canonical Wnt signaling regulates Cdc42 and cell proliferation during tooth root development

Yuanyuan Ma[1,2], Junjun Jing[1], Jifan Feng[1], Yuan Yuan[1], Quan Wen[1], Xia Han[1], Jinzhi He[1], Shuo Chen[1], Thach-Vu Ho[1], and Yang Chai[1*]

1. Center for Craniofacial Molecular Biology, University of Southern California, Los Angeles, CA 90033

2. Guangdong provincial Key Laboratory of Stomatology, Department of Prosthodontics, Guanghua School of Stomatology, Hospital of Stomatology, Sun Yat-sen University, Guangzhou, 510055, PR China

*Corresponding Author

Yang Chai

University Professor

Director

Center for Craniofacial Molecular Biology

University of Southern California

Los Angeles, CA 90033

Tel. (323)442-3480

ychai@usc.edu

Key words: Ror2, tooth root, cell proliferation, Cdc42

Abstract

The control of size and shape is an important part of regulatory process during organogenesis. Tooth formation is a highly complex process that fine-tunes the size and shape of the tooth, which are crucial for its physiological functions. Each tooth consists of a crown and one or more roots. Despite comprehensive knowledge of the mechanism that regulates early tooth crown development, we have limited understanding of the mechanism regulating root patterning and size during development. Here we show that Ror2 mediated non-canonical Wnt signaling in the dental mesenchyme plays a critical role in cell proliferation and thereby regulates root development size in mouse molars. Furthermore, Cdc42 acts as a potential downstream mediator of Ror2 signaling in root formation. Importantly, activation of Cdc42 can restore cell proliferation and partially rescue the root development size defects in *Ror2* mutant mice. Collectively, our findings provide novel insights into the function of Ror2-mediated non-canonical Wnt signaling in regulating tooth morphogenesis and suggest potential avenues for dental tissue engineering.

Introduction

The tooth serves as an important model for investigating the regulatory mechanism of organ morphogenesis. Anatomically, teeth can be divided into two parts: the crown and the root. The development of the crown starts prenatally with early tooth morphogenesis. After crown development is completed, root formation initiates and proceeds through a complex process influenced by Hertwig's epithelial root sheath (HERS), cranial neural crest (CNC)-derived mesenchyme and adjacent anatomical structures (Li et al., 2017). The distribution of proliferation, apoptosis and osteoclast activity in these tissues corresponds with morphological changes during root development (Matalová et al., 2015). To date, we know little about the molecular mechanism that regulates root development size postnatally (Balic and Thesleff, 2015; Li et al., 2017).

Canonical (β-catenin-dependent) Wnt signaling originating from dental mesenchyme and/or epithelium is known to play a crucial role in root patterning and development (Bae et al., 2015; Kim et al., 2013; Lohi et al., 2010; Yamashiro et al., 2007; Yang et al., 2013). Non-canonical (β-catenin-independent) Wnt signaling comprises several pathways that are required for tissue formation and homeostasis (Patel et al., 2019). However, the function of non-canonical Wnt pathways during root development remains unknown.

Receptor tyrosine kinase (RTK)-like orphan receptor 2 (Ror2) is one of the non-canonical Wnt receptors. Ror2 plays significant roles during early embryonic development in several types of tissues, and Ror2 is a potential therapeutic target in cancer due to its association with cancer formation (Debebe and Rathmell, 2015). Ror2 can bind to Wnt5a to contribute to cytoskeletal arrangement, cell migration, cell polarity and cell proliferation, and to modulate downstream gene expression (He et al., 2008; Oishi et al., 2003; Schambony and Wedlich, 2007). Notably, Ror2 can inhibit or activate canonical Wnt signaling at the level of TCF/LEF-mediated transcription depending on whether Wnt ligands are present (Billiard et al., 2005; Mikels and Nusse, 2006). Due to these interesting features including its significance in development and potential for cancer therapy, Ror2 has attracted considerable attention.

In humans, *ROR2* mutations are associated with diseases such as dominant Brachydactyly B (BDB, a shortening of the digits) (Oldridge et al., 2000) and recessive Robinow syndrome (RRS), which is associated with short-limbed dwarfism, abnormal vertebrae, fusion of the ribs, and abnormal facial structures (Afzal and Jeffery, 2003). Interestingly, some individuals with RRS also have dental problems such as fusion of primary teeth, delayed eruption of the permanent teeth and delayed root formation of the permanent teeth, suggesting the involvement of ROR2 in tooth development (Jain et al., 2017). In mice, *Ror2* is expressed in the dental epithelium and mesenchyme at embryonic stages (Lin et al., 2011; Schwabe et al., 2004). *Ror2*$^{-/-}$ mice exhibit retarded crown formation and defective odontoblast differentiation, which are also observed in Wnt5a-deficient mice (Lin et al., 2011). This indicates that Ror2 may participate in mediating Wnt5a signaling during early tooth development. However, roles of ROR2/Ror2 are tissue-specific (Roarty et al., 2017; Sun et al., 2015). Therefore, the questions of whether Ror2 expressed in specific tissues has the capacity to regulate tooth development and whether it modulates root formation remain unclear.

In the present study, we show that crown formation is unaffected in *Ror2* conditional knockout mouse models but loss of *Ror2* in the dental mesenchyme leads to delayed root elongation and ultimately to shortened roots. We further establish that mesenchymal Ror2 regulates cell proliferation, odontoblast differentiation in the apical region of the tooth, and HERS formation through tissue-tissue interactions during postnatal development. Furthermore, we have identified cell division cycle 42 (Cdc42) as a downstream mediator of Ror2 signaling in the regulation of cell proliferation during root development. Importantly, activation of Cdc42 can partially rescue the root development size defect in *Ror2* mutant mice, clearly demonstrating the functional significance of Ror2 and its impact on Cdc42 activation in regulating root development postnatally.

Results

Ror2 in the dental mesenchyme plays a critical role in mouse molar root morphogenesis

Tooth root development begins at around postnatal (PN) 3.5 and completes when the tooth erupts at around PN18.5 (Li et al., 2017). To investigate Ror2's function during molar root development, we investigated its expression pattern at different root development stages. At PN0.5, Ror2 expression was widely distributed in the dental mesenchyme and dental epithelium of wild type mice (Fig. 1A, B) and gradually became more prominent apically in the root-forming region (Fig. 1C-F). The expression of Ror2 was also detectable in the periodontal region and alveolar bone at PN12.5 (Fig. 1G, H). Since the apical dental mesenchyme is closely associated with tooth growth, this enriched apical expression suggests that Ror2 may play a specific role in root development.

To establish the functional significance of Ror2-mediated signaling in tooth development, we generated *Osr2-Cre;Ror2* $^{fl/fl}$ mice with specific ablation of Ror2 in the dental mesenchyme. The expression of Osr2 is detectable in the craniofacial region from E10.5 (Lan et al., 2007) and in the dental mesenchyme from E12.5 (Li et al., 2011). Throughout tooth development, the *Osr2-Cre* transgene targets the dental mesenchyme and the alveolar bone, but not the dental epithelium, in lineage tracing study (Fig. S1A-D). Ror2 expression was undetectable in the dental mesenchyme but still present in the epithelium of *Osr2-Cre;Ror2* $^{fl/fl}$ mice at PN3.5 and PN9.5 (Fig. S1E-H). This expression pattern indicated highly efficient mesenchyme-specific deletion of *Ror2* in *Osr2-Cre;Ror2* $^{fl/fl}$ mice during tooth morphogenesis.

The morphology of the molar tooth crowns in *Osr2-Cre;Ror2* $^{fl/fl}$ mice was similar to that of control molars at PN0.5 and PN2.5 (Fig. S2A-J), prior to root development. We observed no significant differences in cell proliferation or differentiation when comparing the crowns of control and *Osr2-Cre;Ror2* $^{fl/fl}$ molars during this period based on Ki67 immunostaining (Fig. S2K, L), RNAscope of *Dspp* and EdU assay (Fig. S2M, N). Therefore, we concluded that crown patterning is unaffected following the loss of *Ror2* in the dental mesenchyme in *Osr2-Cre;Ror2*$^{fl/fl}$ mice.

We then further compared the tooth root formation of control and *Osr2-Cre;Ror2*$^{fl/fl}$ mice. At PN12.5, the root elongation and furcation formation processes had commenced in the mandibular first molars of control mice (N=4; Fig. 2A-D). However, root elongation was delayed and no furcation had formed in *Osr2-Cre;Ror2* $^{fl/fl}$ molars at this stage (N=4; Fig. 2E-H, U). By PN17.5, the loss of *Ror2* in the dental mesenchyme had resulted in shortened roots, but a normal root number, in mandibular first molars in *Osr2-Cre;Ror2* $^{fl/fl}$ mice (N=4; Fig. 2I-T, V). Histological analysis showed that the dentin formation and alveolar bone formation in the furcation region were disrupted in *Osr2-Cre;Ror2* $^{fl/fl}$ mice compared to controls (Fig. 2Q, T). And the odontoblasts in the furcation region were shorter in *Ror2* mutant molars than those in controls (Fig. 2Q, T). Furthermore, the mandible was smaller in *Osr2-Cre;Ror2* $^{fl/fl}$ mice compared to controls (Fig. 2A, E, I, L, O, R). In order to determine whether the root size defect was caused by loss of *Ror2* in the dental mesenchyme or was secondary to the mandibular bone defect, we collected tooth germs of the mandibular first molars at PN4.5 from *Osr2-Cre;Ror2* $^{fl/fl}$ and control mice and transplanted them into the kidney capsule. After 3 weeks of cultivation, we observed that the *Osr2-Cre;Ror2* $^{fl/fl}$ molars had shortened roots with normal crown formation (N=3; Fig. S3), which is consistent with the phenotype observed *in vivo* and suggests that the root size defect is not secondary to the mandibular defect in *Osr2-Cre;Ror2* $^{fl/fl}$ mice.

Ablation of *Ror2* in the dental mesenchyme disrupts mesenchymal cell proliferation and differentiation

We next evaluated the cellular proliferation activity in the apical region during root development. At PN3.5, there was no obvious difference in the tissue morphology in the apical region between control and *Ror2* mutant molars (Fig. 3A, B, E, F). However, a significant decrease in cell proliferation in the dental mesenchyme of *Osr2-Cre;Ror2* $^{fl/fl}$ molars was observed as we compared Ki67+ (actively cycling) cells in control and *Ror2* mutant mice at PN3.5 (Fig. 3C, D, G, H, Q). Despite this, the proliferation in the root epithelium was not significantly different between *Osr2-Cre;Ror2* $^{fl/fl}$ and control mice (Fig. 3Q). Consistent with this hypo-proliferative cell phenotype in the mesenchyme, we detected significantly reduced expression of S- and M-phase cell cycle markers, suggesting that cell cycle progression was inhibited in *Osr2-Cre;Ror2* $^{fl/fl}$ molars compared to controls (Fig. 3I-P, R, S). Two hours after EdU injection, the number of EdU-labeled cells conducting cDNA synthesis (S phase) was significantly decreased in the

dental mesenchyme of *Osr2-Cre;Ror2* $^{fl/fl}$ mice at PN3.5 (Fig. 3I, J, M, N, R). The expression of PHH3, a marker of mitotic cells, was also reduced in the dental mesenchyme of *Osr2-Cre;Ror2* $^{fl/fl}$ mice (Fig. 3K, L, O, P, S). However, the numbers of EdU-labeled and PHH3-expressing cells were normal in the dental epithelium of *Osr2-Cre;Ror2* $^{fl/fl}$ mice (Fig. 3R, S). Additionally, there was no difference in apoptotic activity in the dental mesenchyme of *Osr2-Cre;Ror2* $^{fl/fl}$ or control mice at PN3.5, PN5.5 and PN9.5 (Fig. S4). This suggests that Ror2 may be required for normal proliferation of dental mesenchymal cells during root development, but not for apoptosis.

A previous study suggested that dental mesenchyme proliferation is crucial for root elongation and for guiding HERS formation during root development (Sohn et al., 2014). We thus investigated the formation of HERS. Morphological changes in HERS were first observed at PN5.5 (Fig. S5A-D), two days later than the cellular defects in the dental mesenchyme of *Osr2-Cre;Ror2* $^{fl/fl}$ mice (Fig. 3). It was particularly obvious that HERS invagination formed a thicker and shorter structure in *Osr2-Cre;Ror2* $^{fl/fl}$ molars at PN7.5 compared to the normal bi-layered structure in the controls (Fig. S5E, F). At PN9.5, HERS lost continuity in both control and *Ror2* mutant molars; in *Ror2* mutant mice, HERS formed a structure that was similar to but shorter than what was seen in the controls (Fig. S5G, H). These findings suggest that loss of *Ror2* in the dental mesenchyme affects the development of HERS through tissue-tissue interaction.

In addition, we investigated the expression of *Dspp*, a marker of terminally differentiated odontoblasts, in *Osr2-Cre;Ror2* $^{fl/fl}$ and control mice at PN9.5. We found no differences in *Dspp* expression throughout the crown region (Fig. 4A, B). However, fewer *Dspp*-positive cells were observed in the apical region below the enamel level in *Osr2-Cre;Ror2* $^{fl/fl}$ mice (Fig. 4C, D). H&E staining showed that dentinogenesis was retarded in the apical region in *Osr2-Cre;Ror2* $^{fl/fl}$ mice (Fig. 4E, F). There was no obvious change in the morphology of odontoblasts or preodontoblasts in *Ror2* mutant mice. In comparing them to a detailed published description of odontoblasts in the apical root region (Bae et al., 2013), we found that cells in the transition zone from preodontoblasts to odontoblasts showed a looser alignment in *Osr2-Cre;Ror2* $^{fl/fl}$ molars compared to a condensed, columnar alignment in control molars (yellow asterisks; Fig. 4G, H). These results indicated that loss of *Ror2* in the dental mesenchyme disrupts differentiation of

odontoblasts and dentinogenesis during root elongation, eventually resulting in the phenotypes observed at PN12.5 and PN17.5 (Fig. 2).

Ror2 in the dental epithelium is not required for root development

Ror2 is expressed in the dental epithelium as well as in the mesenchyme in mouse molars (Fig. 1). To investigate whether epithelial Ror2 is crucial for root formation, we generated *K14-rtTA;Teto-Cre;Ror2* $^{fl/fl}$ mice, in which *Ror2* is ablated in the dental epithelium at PN3.5 (Fig. S6A-D). Based on microCT images and H&E staining, we found no significant differences in root length or root number between *K14-rtTA;Teto-Cre;Ror2* $^{fl/fl}$ and control mice at PN21.5 (Fig. S6E-L). These findings indicated that epithelial Ror2 is not required for root formation.

Activation of Cdc42 partially rescues root development and restores mesenchymal cell proliferation in *Ror2* mutant mice

It has been reported that Ror2 participates in both canonical and non-canonical Wnt signaling (Billiard et al., 2005; He et al., 2008). For example, Ror2 has been identified as a regulator of canonical Wnt signaling that affects the stabilization of cytosolic β-catenin *in vivo* and *in vitro* (Billiard et al., 2005; Mikels and Nusse, 2006; Roarty et al., 2017). Thus, we assessed the expression of *Axin2* and active β-catenin in the dental mesenchyme of the mandibular first molars. We found no significant differences between *Osr2-Cre;Ror2* $^{fl/fl}$ and control molars at PN3.5 (Fig. S7A-D, I), which indicated that canonical Wnt signaling is not involved in the decreased cell proliferation caused by loss of *Ror2* in the dental mesenchyme. On the other hand, it has been shown that Ror2-mediated non-canonical Wnt signaling leads to transcriptional responses via c-Jun and ATF2 in *Xenopus* (Schambony and Wedlich, 2007). However, there were no distinguishable differences in the expression of phospho-c-Jun or phospho-ATF2 between *Osr2-Cre;Ror2* $^{fl/fl}$ and control molars at PN3.5 (Fig. S7E-H). The activation of the small GTPase Rac1, an upstream mediator of c-Jun and ATF2, was also unchanged in the Ror2 mutant mice (Fig. S7J). Our results indicated that Ror2-mediated signaling did not trigger the activation of c-Jun and ATF2 in mouse molar root context. Due to the complexity of non-canonical Wnt pathways and the context-dependent function of Ror2, we hypothesized that Ror2 may regulate tooth root development via other mediators of non-canonical Wnt signaling.

To further probe the molecular mechanism of Ror2-mediated signaling in regulating root development, we analyzed gene expression profiles and performed pathway enrichment analysis in the dental mesenchyme using RNA-seq from *Osr2-Cre;Ror2* $^{fl/fl}$ and control mice at PN3.5 (Fig. 5A, B; Table S2, S3). We identified 891 genes that were differentially expressed in *Osr2-Cre;Ror2* $^{fl/fl}$ versus control mice (Table S3). These genes segregated into two groups shown in the heat map in Fig. 5A, and interesting candidate genes related to cell proliferation are listed in Table.S2.

Pathway enrichment analysis showed that genes related to regulation of eIF4 and p70S6K signaling were among the most enriched categories and therefore the most likely to contribute to the root size defect in *Ror2* mutant mice (Fig. 5B). The p70S6 kinase (p70S6K, S6K1) is crucially important in protein synthesis, cell growth and cell proliferation (Harada et al., 2001). Therefore, we tested the level of p70S6K in the dental mesenchyme of *Osr2-Cre;Ror2* $^{fl/fl}$ and control mice. The results showed that the phosphorylation of p70S6K was significantly decreased in *Osr2-Cre;Ror2* $^{fl/fl}$ mice compared to controls (Fig. 5C, D), which is consistent with the signaling pathway analysis. p70S6K is usually regarded as a key factor downstream of mTOR pathway (Harada et al., 2001). Surprisingly, there was no decrease in the phosphorylation of mTOR in *Ror2* mutant mice (Fig. 5C, D), which indicates that the inactivation of p70S6K may be independent of mTOR signaling in *Osr2-Cre;Ror2* $^{fl/fl}$ mouse molars. p70S6K has also been identified as a downstream effector of Cdc42 (Chou and Blenis, 1996), a small Rho-family GTPase. Cdc42's function is typically dependent on its switching between an active, GTP-bound form and an inactive GDP form. Non-canonical Wnt pathway is important for Cdc42 signaling (Carvalho et al., 2019), and Cdc42 is required for cell cycle progression (Chou et al., 2003). Therefore, we firstly tested the level of GTP-Cdc42 protein in tissue lysates at PN3.5 (Fig. 5E). The small G-protein activation assay showed that Cdc42 activation was significantly decreased in *Osr2-Cre;Ror2* $^{fl/fl}$ mouse molars in both equalized protein concentrations (0.15μg/μl and 0.61μg/μl) (Fig. 5E). We then examined the expression pattern of *Cdc42* in the mouse molar at PN3.5. The results showed that there was an overlap in the expression of *Cdc42* and Ki67 in the apical region of the molar root (Fig. 5F, G, G', G''), and in the same region there was also overlapping expression between *Cdc42* and Ror2 (Fig. 5H). Furthermore, the dental mesenchymal cells showed a decrease in cell proliferation after treatment with ZCL278 (50 μM),

a Cdc42 inhibitor, for 20 h *in vitro* (Fig. S8A-C). These results indicated that Cdc42 may mediate the function of Ror2 in cell proliferation during root development.

Before proceeding with further mechanistic studies, we analyzed gene expression profiles and found that several cell cycle-promoting genes had reduced expression levels in *Osr2-Cre;Ror2* $^{fl/fl}$ mice compared to controls (Table S2). Cyclin E1 (Ccne1) and Cyclin A2 (Ccna2) are important regulators of the G1/S transition and S phase of cell cycle progression, respectively (Sonntag et al., 2018). We confirmed that there was a significant reduction in the expression of *Ccne1* and *Ccna2* in the apical mesenchyme *in vivo* at PN3.5 by *in situ* hybridization and qPCR (Fig. 5I-R). It indicated that loss of *Ror2* in the dental mesenchyme leads to the down-regulation of *Ccne1* and *Ccna2* during root development. Furthermore, we also detected the decreased expression of *Ect2*, which is reported to be related to mitosis, in *Osr2-Cre;Ror2* $^{fl/fl}$ molars (Fig. S8C-G). These results were likely associated with the decrease in Edu-labeled cells and PHH3-positive cells seen in the dental mesenchyme of *Osr2-Cre;Ror2* $^{fl/fl}$ molars (Fig. 3I, J, M, N, R). It has been argued that Cdc42's function in cell cycle regulation is to promote G1 progression through the induction of *Ccne1* expression (Chou et al., 2003). Therefore, the reduced Cdc42 activation signal observed at PN3.5 suggests that Cdc42 may participate in Ror2-induced *Ccne1* expression in tooth root context.

Cdc42 is the convergence point between the gene expression profiling and pathway enrichment analyses we conducted. Considering that Cdc42 is involved in non-canonical Wnt signaling and plays an important role in cell cycle regulation (Chou et al., 2003; Olson et al., 1995), we hypothesized that Cdc42 may be an important downstream mediator of Ror2 signaling in regulating root development. To test this hypothesis, we first investigated whether Cdc42 activator could rescue root growth in *Osr2-Cre;Ror2* $^{fl/fl}$ mice. We collected tooth germs from control and *Osr2-Cre;Ror2* $^{fl/fl}$ mice at PN4.5 and transplanted them with BSA-soaked beads or activator-soaked beads into the kidney capsule. After 3 weeks of cultivation, we harvested the molars for analysis. Based on microCT images and H&E staining, the shortened roots of *Osr2-Cre;Ror2* $^{fl/fl}$ molars were partially rescued by Cdc42 activator treatment compared to the controls treated with BSA or activator (N=4; Fig. 6A-L). However, BSA-soaked beads had no significant effect on the root defect in *Osr2-Cre;Ror2* $^{fl/fl}$ molars (N=3; Fig. 6M-P). Furthermore,

the odontoblasts in the furcation region of *Ror2* mutant molars treated with Cdc42 activator appeared longer than those in the mutant molars treated with BSA beads, and were similar in size to those in the control molars (Fig. 6D, D', H, H', L, L', P, P'). In order to investigate whether the cellular defect was rescued, we examined cell proliferation activity in the apical region at an early stage. It has been reported that the rescue of gene expression can occur after 2 days of incubation with protein-soaked beads in organ culture (Huang et al., 2010). Therefore, we collected samples 3 days after transplantation under the kidney capsule for analysis in cellular level. We found that the numbers of Ki67- and PHH3-positive cells were higher in activator-treated *Osr2-Cre;Ror2* $^{fl/fl}$ molars than in BSA-treated *Ror2* mutant molars (Fig. 7A-N). However, there was no statistical difference in Ki67/PHH3-positive cells between activator-treated and BSA-treated controls (Fig. 7E-N). This may explain why there was normal root formation in activator-treated control molars after 3 weeks of cultivation under the kidney capsule. Additionally, p70S6K was also activated with higher phosphorylation in activator-treated *Osr2-Cre;Ror2* $^{fl/fl}$ molars compared to BSA-treated *Ror2* mutant molars (Fig. 7O). Furthermore, the expression pattern of *Cdc42* and Ki67 in wild type tooth germ was similar to that at PN7.5 *in vivo* (Fig. S8I-L). Therefore, we concluded that activation of Cdc42 contributes to the restoration of cell proliferation in the apical region and root formation in *Osr2-Cre;Ror2* $^{fl/fl}$ molars. These results highlight the significance of Cdc42 as an effective mediator of Ror2 in regulating cell proliferation during root morphogenesis.

Discussion

Previous studies have reported that several signaling pathways, including BMP, TGFβ, WNT, FGF and SHH, are important in regulating root formation. The function of non-canonical Wnt signaling in root development, however, has remained unknown. Ror2 crucially regulates the morphogenesis of a variety of organs during embryonic development (Minami et al., 2010). Here, we have provided evidence that Ror2 plays a crucial role in regulating cell proliferation in the apical region of the mouse molar, and consequently in regulating root size during development. Additionally, we identified Cdc42 as a potential downstream mediator of Ror2 signaling in root formation associated with mesenchymal cell proliferation during postnatal tooth morphogenesis.

Mesenchymal Ror2 mediates epithelial-mesenchymal interactions during root development

Sequential, reciprocal epithelial-mesenchymal interactions are crucial for virtually every aspect of tooth morphogenesis and development (Balic and Thesleff, 2015). Both epithelial and mesenchymal cells contribute to forming the tooth root (Li et al., 2017). Previous studies have shown that HERS is important for the induction of odontoblast differentiation (Kim et al., 2013) and may be responsible for determining tooth root size, shape and number (Li et al., 2017). On the molecular level, HERS secretes Shh under the control of TGFβ/BMP/SMAD, and in so doing regulates mesenchymal *Nfic* expression to control root elongation (Huang et al., 2010), suggesting that HERS acts as a signaling center that mediates epithelial-mesenchymal interactions. Some signaling molecules in the dental mesenchyme are also essential for HERS formation as well as for root formation. For example, conditional knockout of *β-catenin* or *Tgfbr2* in odontoblasts disrupts root odontoblast differentiation and HERS formation, which leads to molar root defects (Kim et al., 2013; Wang et al., 2013). In this study, we provide support for the notion that *Ror2* is not required in the dental epithelium during root formation, but mesenchyme-specific deletion of *Ror2* results in shortened roots in *Osr2-Cre;Ror2* $^{fl/fl}$ mice, suggesting that Ror2-mediated signaling is specifically required in the dental mesenchyme during root development.

Soon after birth, *Osr2-Cre;Ror2* $^{fl/fl}$ mice exhibit decreased mesenchymal proliferation, followed by HERS malformation with a less distinct invagination into the mesenchyme and disrupted odontoblast differentiation. A previous study has shown that spatial regulation of mesenchymal proliferation is required for root patterning, and that this process may involve the mesenchyme forming a physical structure that affects the epithelial invagination of HERS (Sohn et al., 2014). In light of this, we suggest that the HERS malformation seen in *Osr2-Cre;Ror2* $^{fl/fl}$ mice may be caused at least in part by the physical effect of the dental mesenchyme resulting from its altered proliferation. Other factors secreted from the dental mesenchyme may also have affected HERS formation through tissue-tissue interactions. Although it is still unknown how HERS formation is specifically affected in *Ror2* mutant mice, the evidence suggests that mesenchymal Ror2 is important for modulating epithelial-mesenchymal interactions during root development. We found different morphological changes to odontoblasts in the elongation and furcation regions of

the root. These differences may result from the site-specific regulation of *Ror2* or from the distinct mechanisms underlying root elongation and furcation formation. For example, *Osx*^{Col} and *Osx*^{OC} mice have also been reported to form short roots with extremely thin interradicular dentin (Kim et al., 2015). In *Osr2-Cre;Ror2* $^{fl/fl}$ mice, the disrupted differentiation of odontoblasts in the elongation region may be related to decreased mesenchymal proliferation causing fewer cells to withdraw from the cell cycle for differentiation.

Ror2-Cdc42 signaling regulates root development

Although Ror2 can mediate canonical Wnt pathway (Billiard et al., 2005; Roarty et al., 2017), we show that loss of *Ror2* in the dental mesenchyme has no effect on β-catenin-dependent transcriptional activity when tooth root development initiates. Therefore, we have focused on Ror2-mediated non-canonical Wnt signaling in our mechanistic study, specifically the function of Cdc42 activated by Ror2 in root formation.

CDC42 mutations result in a spectrum of human diseases with various clinical phenotypes, such as developmental delay, growth retardation, facial dysmorphism and more (Szczawinska-Poplonyk et al., 2020). In mouse models, epithelial Cdc42 deletion induces enamel defects and dental cystogenesis, suggesting it may play a role in tooth development (Melendez et al., 2013). Cdc42 is essential in various cellular processes. For example, non-canonical Wnt-dependent Cdc42 activity is required for tissue repair after neural demyelination injury (Chavali et al., 2018). The Ror2-Cdc42 signaling axis has also been reported to mediate Wnt5a signaling transduction to regulate junctional mechano-coupling between endothelial cells (Carvalho et al., 2019). Interestingly, deletion of *Cdc42* in the neural crest (NC) results in multiple defects in NC derivatives because of reduced mitotic activity (Fuchs et al., 2009). In our study, deletion of *Ror2* in the dental mesenchyme results in decreased Cdc42 activity and cell proliferation in *Osr2-Cre;Ror2* $^{fl/fl}$ mice. Cdc42 activator can restore cell proliferation in the apical region of mouse molars and partially rescue the shortened root phenotype in *Ror2* mutant mice. These findings imply that Cdc42 is a key downstream mediator of Ror2 signaling during root development.

Ror2 regulates Cdc42 activation through Phosphoinositide 3 kinase, as has been described in *Xenopus* gastrulation (Schambony and Wedlich, 2007). It has also been reported that Cdc42 acts downstream of the Ca^{2+} signaling pathway triggered by Wnt5a binding to the Ror2-Frizzled receptor complex (Jin et al., 2005; Li et al., 2009; Zhan et al., 2016). In our study, pathway enrichment analysis has shown that Ca^{2+} signaling is downregulated in *Ror2* mutant mice. We also detect the decreased expression of calcineurin A (a downstream mediator of Ca^{2+} signaling) and transcription factor *Nfatc4* in the apical region of mouse molars, confirming the down-regulation of Ca^{2+} signaling in *Osr2-Cre;Ror2* $^{fl/fl}$ mice. It remains to be investigated whether altered Ca^{2+} signaling caused by loss of *Ror2* in the dental mesenchyme plays an important role in modulating the activity of Cdc42 to regulate root size during tooth morphogenesis.

Consistent with the inhibition of Cdc42 activity in *Osr2-Cre;Ror2* $^{fl/fl}$ mice, the phosphorylation of p70S6K, an effector of Cdc42, is significantly decreased in the dental mesenchyme. Consistent with this finding, p70S6K activity has been increased after Cdc42 activator treatment. The phosphorylation of p70S6K is beneficial for protein synthesis required both to enter the cell cycle (G1 phase) from G0 and to proceed to S phase (Pearson and Thomas, 1995). Therefore, the cell proliferation in the apical region is restored after Cdcd42/p70S6K is activated in *Ror2* mutant molars. Although it is well documented that p70S6K is a downstream target of mTOR pathway, this is not the case in *Ror2* mutant mice during tooth root development. *In vitro* study has shown that Cdc42 can act through both mTOR-dependent and -independent pathways to regulate p70S6K in HEK293 cells (Fang et al., 2003). Therefore, we suggest that the lack of the upstream signal from Ror2 results in de-phosphorylation and inactivation of p70S6K in the dental mesenchyme, where it may be independent of mTOR pathway but requires the involvement of Cdc42. It has also been reported that Cdc42 has multiple functions in regulating the cell cycle (Chou et al., 2003; Olson et al., 1995); for example, it can regulate mitosis via modulating chromosome alignment (Yasuda et al., 2006). Therefore, the Cdc42-p70S6K axis may not be the only pathway associated with Cdc42 in regulating cell proliferation in the dental mesenchyme. We cannot exclude other ways in which Cdc42 functions in cell cycle regulation. Collectively, our findings indicate that Cdc42 is an important downstream target of Ror2 signaling that effectively modulates cell proliferation during root development.

In summary, our study demonstrates that Ror2-mediated signaling pathway in the dental mesenchyme plays a crucial role in regulating molar root development via Cdc42 activation. However, loss of *Ror2* in the dental epithelium does not affect root development. Our findings suggest that Ror2 signaling is tissue-specific during root morphogenesis. Importantly, the shortened root size caused by loss of *Ror2* in the dental mesenchyme is similar to the dental problems seen in some individuals with RRS who have mutations in *ROR2* (Jain et al., 2017). The sequences of mouse and human *Ror2/ROR2* are almost identical (Stricker et al., 2017). Therefore, a better understanding of the underlying mechanism involved in mouse tooth root development could shed light on the dental defects seen in patients and suggests potential avenues for future root regeneration.

Materials and methods

Generation of transgenic mouse lines

Osr2-Cre mice were a gift from Rulang Jiang (Cincinnati Children's Hospital) (Lan et al., 2007). *K14-rtTA* (JAX#007678) (Xie et al., 1999), *Teto-Cre* (JAX#006234) (Perl et al., 2002), *Ror2*$^{fl/fl}$ (JAX#018354) (Ho et al., 2012), and *ROSA26*$^{loxP\text{-}STOP\text{-}loxP\text{-}\ tdTomato}$ (*tdTomato* conditional reporter, JAX#007905) (Madisen et al., 2010) mouse lines were purchased from The Jackson Laboratory. *Osr2-Cre;Ror2*$^{fl/+}$ male mice were crossed with *Ror2*$^{fl/fl}$ female mice to generate *Osr2-Cre;Ror2*$^{fl/fl}$ mice. *K14-rtTA;Teto-Cre;Ror2*$^{fl/fl}$ male mice were crossed with *K14-rtTA;Ror2*$^{fl/fl}$ female mice to generate *K14-rtTA;Teto-Cre;Ror2*$^{fl/fl}$ mice. Doxycycline rodent diet was administered every day from E14.5. All animal studies were approved by the Institutional Animal Care and Use Committee (IACUC) at the University of Southern California.

Kidney capsule transplantation

Kidney capsule transplantation was performed as described previously (Oka et al., 2007). After genotyping, the tooth germs of the mandibular first molars were collected from PN4.5 *Ror2*$^{fl/fl}$ control or *Osr2-Cre;Ror2*$^{fl/fl}$ mice. Each tooth germ was surgically transplanted under the kidney capsule of a host mouse. The explants were harvested after 21 days. For the rescue experiment, affi-Gel blue agarose beads (Bio-rad, Hercules, CA, USA) were soaked in bovine serum albumin (BSA) (100 μg/ml) or the Cdc42 activator (50 μg/ml; Cytoskeleton, Inc. Denver, CO, USA) overnight at 4°C prior to use. After that, BSA and activator beads were transplanted into the

kidney capsule with the tooth germ collected from *Ror2*$^{fl/fl}$ control or *Osr2-Cre;Ror2*$^{fl/fl}$ mouse mandibles at PN4.5. The explants were collected after 2, 3 or 21 days.

MicroCT analysis

MicroCT analysis was performed using a SCANCO µCT50 device at the University of Southern California Molecular Imaging Center. The microCT images were acquired with the X-ray source at 70kVp and 114µA. The data were collected at a resolution of 16.7µm. Three-dimensional (3D) reconstruction was done with AVIZO 7.1 (Visualization Sciences Group).

Histological analysis

Samples were dissected and fixed in 4% paraformaldehyde overnight at 4°C and decalcified in 10% EDTA (PH=7.5) at 4°C for 1-3 weeks depending on the age of samples. Then samples were processed into paraffin-embedded serial sections at 5 µm using a microtome (Leica). For general morphology, deparaffinized sections were stained with Hematoxylin and Eosin (H&E) using standard procedures.

For cryosections, decalcified samples were dehydrated in 15% and 60% sucrose/DEPC-treated PBS solution overnight at 4°C. Samples were then embedded in OCT compound (Tissue-Tek, Sakura). Embedded samples were then cryo-sectioned at 8µm thickness using a cryostat (Leica CM1850).

Immunostaining

Immunostaining was carried out using the primary antibodies against Ror2 (1:100, Cell Signaling, #886395), Ki67 (1:100, Abcam, ab15580), K14 (1:200, Abcam, ab181595), Amelogenin X (AMELX, 1:200, Abcam, ab153915), phospho-ATF2 (1:100, Abcam, Ab32019), Phospho-c-Jun (1:100, Abcam, ab30620), phospho-Histone H3 (1:100, Millipore Sigma, 06-570) and active β-catenin (1:100, Cell Signaling, #19807s). Alexa™ Fluor 647, Alexa™ Fluor 568, Alexa™ Fluor 488(1:200, Invitrogen) and Alexa Fluor™ 488 tyramide super boost™ kit (B40922, Invitrogen) were used for detection. Sections were counterstained with DAPI.

In situ hybridization

In situ hybridization was carried out following standard procedure using RNAscope® 2.5 HD Reagent Kit-RED(322350, ACDBio) and RNAscope® Multiplex fluorescent reagent kit V2 Assay (323100-USM, ACDBio). All probes from mouse cDNA clones were purchased from ACDBio including RNAscope® Probe-Mm-*Dspp* (448301), - *Cdc42* (473041), -*Ccne1* (503801), -*Ccna2-C3* (442661-C3), -*Ect2* (502121) and -*Axin2* (400331).

Western blotting

Dental pulp of the mandibular first molars was dissected from *Ror2*$^{fl/fl}$ control mice and *Osr2-Cre;Ror2*$^{fl/fl}$ mice at PN3.5. For kidney capsule transplantation, dental pulp of transplanted molars was dissected from the kidney capsule 2 days post-surgery. For western blotting, tissues were lysed in lysis buffer [50 mMTris-HCl (pH 7.5), 150 mM NaCl, 2 mM EDTA, 0.1% NP-40, 10% glycerol and protease inhibitor cocktail] and protein fractions were isolated. Proteins were separated on 4-15% protein gels (Bio-Rad) and transferred to 0.2 µm PVDF membrane. Membranes were blocked in 5% BSA for 1 h at room temperature and then incubated with primary antibody overnight at 4°C followed by 1h incubation with HRP-conjugated anti-mouse or anti-rabbit secondary antibody. Immunoreactive protein was detected using SuperSignal™ West Femto Maximum Sensitivity Substrate (Thermo Fisher Scientific, A10044).

The primary antibodies used for western blotting were as follows: anti-GAPDH (1:1000, Cell Signaling, #5174s); anti-Ror2 (1:1000, Cell Signaling, #886395); anti-Cdc42 (1:1000, Abcam, Ab64533); anti-phospho-p70S6 kinase (1:1000, Cell Signaling, #9205S); anti-p70S6K (1:1000, Cell Signaling, #2708); anti-mTOR (1:1000, Cell Signaling, #2972s); and anti-phospho-mTOR (1:1000, Invitrogen, 44-1125G).

Cdc42/Rac1 G-LISA activation assay

Dental pulp of the mandibular first molars was dissected from *Ror2*$^{fl/fl}$ control mice and *Osr2-Cre;Ror2*$^{fl/fl}$ mice at PN3.5. Then tissues were lysed in lysis buffer including protease inhibitor cocktail (Cytoskeleton, #PIC02) and protein fractions were isolated. According to the recommended protocol, GTP-loaded Cdc42 or Rac1 protein in tissue lysates was detected using Cdc42 or Rac1 G-LISA assay, respectively (Cytoskeleton, #BK127/BK128). The level of activation was measured by reading at OD490nm.

TUNEL assays

Apoptotic cells in mouse molars were detected using the Click-iT® Plus TUNEL assay (Thermo Fisher, C10617) according to the recommended protocol.

EdU incorporation and staining

To test cell proliferation, the *Ror2*$^{fl/fl}$ control and *Osr2-Cre;Ror2*$^{fl/fl}$ mice were treated with a 2-hour pulse of EdU (25ug/g body weight) administered intraperitoneally (I.P.) at PN3.5. For cell differentiation analysis, EdU was injected I.P. at PN0.5 and samples were collected at PN2.5. Specimens were fixed, decalcified, and sectioned as described for histological analysis. EdU was

detected using a Click-iT™ Plus EdU Cell Proliferation Kit (Thermo Fisher, C10637). Sections were counterstained with DAPI.

RNA sequencing (RNA-seq) analysis

Dental pulp of the mandibular first molar was dissected out from *Ror2*$^{fl/fl}$ control mice and *Osr2-Cre;Ror2*$^{fl/fl}$ mice at PN3.5. RNA was then extracted using Rneasy® Micro kit (Qiagen). cDNA library preparation and sequencing were performed at the UCLA Technology Center for Genomics & Bioinformatics. A total of 200 million single-end reads with 75 cycles were performed on Illumina Hiseq 4000 equipment for three pairs of samples. High-quality reads were aligned using TopHat 2 with the mm10 genome. Data were quantitated by counting the number of reads over exons and normalized using RPKM. Differential expression was estimated by selecting transcripts that changed with a significance of p <0.05.

Cell culture *in vitro* assay

The apical half of the dental pulp mesenchyme of the mandibular first molar was dissected out from wild type mice at PN3.5. The tissue was minced, centrifuged and re-suspended in α-MEM with 20% FBS, 2mM L-glutamine, 55 μM 2-mercaptoethanol, 100 U/ml penicillin and 100 μg/ml streptomycin (Life Science Technologies). After 5 days of cultivation, cells were digested and obtained by passing through a 40 um strainer (Corning). The cell suspension was seeded at 3.5×10^4/well in 12-well plate culture (Corning) and incubated for 48 h at 37 °C with 5% O_2 and 5% CO_2. The medium was then changed using fresh α-MEM without FBS for 10 h. Serum-starved mesenchymal cells were then incubated for another 20 h with DMSO as control or 50 μM ZCL278 (Cdc42 inhibitor; Tocrs, #4794). For detection of PHH3, cells were washed with PBS before fixation with 4% PFA in PBS at RT for 20 min. Antibody to PHH3 was used at 1:100 dilution. Alexa™ Fluor 647 was used for detection. Samples were counterstained with DAPI.

Quantitative (q) PCR analysis

RNA was isolated from the dental pulp of the mandibular first molars from *Ror2*$^{fl/fl}$ control mice and *Osr2-Cre;Ror2*$^{fl/fl}$ mice at PN3.5 using Rneasy® Micro kit (Qiagen). iScript™ cDNA Synthesis Kit (Bio-Rad) was used for cDNA synthesis. qPCR was then performed on an iCycler (Bio-Rad) with gene-specific primers and SYBR Green using SsoFast™ EvaGreen® Supermix kit (Bio-Rad). Values were normalized to *Gapdh* using the $2^{-\Delta\Delta Ct}$ method. The PCR primers are shown in Table S1.

Statistical analysis

Data are presented as mean ± SEM and were analyzed using Prism 8 (GraphPad Software). N number represents the number of control or mutant mice or of independent experiments performed. We used $N \geq 3$ for all experiments unless otherwise noted. For each independent experiment including qPCR and Western blotting, at least three technical replicates were analyzed. For immunostaining and *in situ* hybridization, we used samples from at least three individual mice and representative images from one of three sections of one sample are shown. For *in vivo* study, statistical comparisons were performed using Student's *t* test. For *ex-vivo* study, statistical significance was determined using two-way analysis of variance (ANOVA), followed by Tukey's multiple comparison tests. $P < 0.05$ was considered statistically significant for all analyses.

Acknowledgements

We thank Bridget Samuels and Linda Hattemer for critical reading of the manuscript. We thank USC Libraries Bioinformatics Services for assisting with data analysis. The bioinformatics software and computing resources used in the analysis are funded by the USC Office of Research and the USC Libraries.

Competing interests

The authors declare no competing or financial interests.

Funding

This work was supported by the National Institute of Dental and Craniofacial Research, National Institutes of Health (R01 DE022503, R01 DE012711, U01 DE028729 to Yang Chai).

References

Afzal, A. R. and Jeffery, S. (2003). One gene, two phenotypes: ROR2 mutations in autosomal recessive Robinow syndrome and autosomal dominant brachydactyly type B. *Human Mutation* **22**, 1-11.

Bae, C.-H., Kim, T.-H., Chu, J.-Y. and Cho, E.-S. (2013). New population of odontoblasts responsible for tooth root formation. *Gene Expression Patterns* **13**, 197-202.

Bae, C. H., Kim, T. H., Ko, S. O., Lee, J. C., Yang, X. and Cho, E. S. (2015). Wntless regulates dentin apposition and root elongation in the mandibular molar.

Balic, A. and Thesleff, I. (2015). Chapter Seven - Tissue Interactions Regulating Tooth Development and Renewal. In *Current Topics in Developmental Biology* (ed. Y. Chai), pp. 157-186: Academic Press.

Billiard, J., Way, D. S., Seestaller-Wehr, L. M., Moran, R. A., Mangine, A. and Bodine, P. V. N. (2005). The Orphan Receptor Tyrosine Kinase Ror2 Modulates Canonical Wnt Signaling in Osteoblastic Cells. *Molecular Endocrinology* **19**, 90-101.

Carvalho, J. R., Fortunato, I. C., Fonseca, C. G., Pezzarossa, A., Barbacena, P., Dominguez-Cejudo, M. A., Vasconcelos, F. F., Santos, N. C., Carvalho, F. A. and Franco, C. A. (2019). Non-canonical Wnt signaling regulates junctional mechanocoupling during angiogenic collective cell migration. *Elife* **8**, e45853.

Chavali, M., Klingener, M., Kokkosis, A. G., Garkun, Y., Felong, S., Maffei, A. and Aguirre, A. (2018). Non-canonical Wnt signaling regulates neural stem cell quiescence during homeostasis and after demyelination. *Nature Communications* **9**, 36.

Chou, M. M. and Blenis, J. (1996). The 70 kDa S6 Kinase Complexes with and Is Activated by the Rho Family G Proteins Cdc42 and Rac1. *Cell* **85**, 573-583.

Chou, M. M., Masuda-Robens, J. and Gupta, M. L. (2003). Cdc42 promotes G1 progression through p70 S6 kinase-mediated induction of cyclin E expression. *Journal of Biological Chemistry* **278**, 35241-35247.

Debebe, Z. and Rathmell, W. K. (2015). Ror2 as a Therapeutic Target in Cancer. *Pharmacology & Therapeutics* **150**, 143-148.

Fang, Y., Park, I.-H., Wu, A.-L., Du, G., Huang, P., Frohman, M. A., Walker, S. J., Brown, H. A. and Chen, J. (2003). PLD1 Regulates mTOR Signaling and Mediates Cdc42 Activation of S6K1. *Current Biology* **13**, 2037-2044.

Fuchs, S., Herzog, D., Sumara, G., Büchmann-Møller, S., Civenni, G., Wu, X., Chrostek-Grashoff, A., Suter, U., Ricci, R., Relvas, J. B., et al. (2009). Stage-Specific Control of Neural Crest Stem Cell Proliferation by the Small Rho GTPases Cdc42 and Rac1. *Cell stem cell* **4**, 236-247.

Harada, H., Andersen, J. S., Mann, M., Terada, N. and Korsmeyer, S. J. (2001). p70S6 kinase signals cell survival as well as growth, inactivating the pro-apoptotic molecule BAD. *Proceedings of the National Academy of Sciences* **98**, 9666.

He, F., Xiong, W., Yu, X., Espinoza-Lewis, R., Liu, C., Gu, S., Nishita, M., Suzuki, K., Yamada, G., Minami, Y., et al. (2008). Wnt5a regulates directional cell migration and cell proliferation via Ror2-mediated noncanonical pathway in mammalian palate development. *Development (Cambridge, England)* **135**, 3871-3879.

Ho, H.-Y. H., Susman, M. W., Bikoff, J. B., Ryu, Y. K., Jonas, A. M., Hu, L., Kuruvilla, R. and Greenberg, M. E. (2012). Wnt5a-Ror-Dishevelled signaling constitutes a core developmental pathway that controls tissue morphogenesis. *Proceedings of the National Academy of Sciences of the United States of America* **109**, 4044-4051.

Huang, X., Xu, X., Bringas, P., Jr., Hung, Y. P. and Chai, Y. (2010). Smad4-Shh-Nfic signaling cascade-mediated epithelial-mesenchymal interaction is crucial in regulating tooth root development. *Journal of bone and mineral research : the official journal of the American Society for Bone and Mineral Research* **25**, 1167-1178.

Jain, P. S., Gupte, T. S., Jetpurwala, A. M. and Dedhia, S. P. (2017). Robinow Syndrome and Fusion of Primary Teeth. *Contemp Clin Dent* **8**, 479-481.

Jin, M., Guan, C. B., Jiang, Y. A., Chen, G., Zhao, C. T., Cui, K., Song, Y. Q., Wu, C. P., Poo, M. M. and Yuan, X. B. (2005). Ca2+-Dependent Regulation of Rho GTPases Triggers Turning of Nerve Growth Cones. *The Journal of Neuroscience* **25**, 2338.

Kim, T. H., Bae, C. H., Lee, J. C., Kim, J. E., Yang, X., de Crombrugghe, B. and Cho, E. S. (2015). Osterix regulates tooth root formation in a site-specific manner. *Journal of dental research* **94**, 430-438.

Kim, T. H., Bae, C. H., Lee, J. C., Ko, S. O., Yang, X., Jiang, R. and Cho, E. S. (2013). beta-catenin is required in odontoblasts for tooth root formation. *Journal of Dental Research* **92**, 215-221.

Lan, Y., Wang, Q., Ovitt, C. E. and Jiang, R. (2007). A unique mouse strain expressing Cre recombinase for tissue-specific analysis of gene function in palate and kidney development. *genesis* **45**, 618-624.

Li, J., Huang, X., Xu, X., Mayo, J., Bringas, P., Jiang, R., Wang, S. and Chai, Y. (2011). SMAD4-mediated WNT signaling controls the fate of cranial neural crest cells during tooth morphogenesis. *Development (Cambridge, England)* **138**, 1977.

Li, J., Parada, C. and Chai, Y. (2017). Cellular and molecular mechanisms of tooth root development. *Development (Cambridge, England)* **144**, 374-384.

Li, L., Hutchins, B. I. and Kalil, K. (2009). Wnt5a Induces Simultaneous Cortical Axon Outgrowth and Repulsive Axon Guidance through Distinct Signaling Mechanisms. *The Journal of Neuroscience* **29**, 5873.

Lin, M., Li, L., Liu, C., Liu, H., He, F., Yan, F., Zhang, Y. and Chen, Y. (2011). Wnt5a regulates growth, patterning, and odontoblast differentiation of developing mouse tooth. *Developmental Dynamics* **240**, 432-440.

Lohi, M., Tucker, A. S. and Sharpe, P. T. (2010). Expression of Axin2 indicates a role for canonical Wnt signaling in development of the crown and root during pre- and postnatal tooth development. *Developmental Dynamics* **239**, 160-167.

Madisen, L., Zwingman, A., T., Sunkin, S. M., Oh, S. W., Zariwala, H. A., Gu, H., Ng, L. P., Richard D., Hawrylycz, M. J., Jones, A. R., et al. (2010). A robust and high-throughput Cre reporting and characterization system for the whole mouse brain. *Nat Neurosci* **13**, 133-140.

Martin, T. D., Dennis, M. D., Gordon, B. S., Kimball, S. R. and Jefferson, L. S. (2014). mTORC1 and JNK coordinate phosphorylation of the p70S6K1 autoinhibitory domain in skeletal muscle following functional overloading. *Am J Physiol Endocrinol Metab.* **306**, E1397-1405.

Matalová, E., Lungová, V. and Sharpe, P. (2015). Chapter 26 - Development of Tooth and Associated Structures. In *Stem Cell Biology and Tissue Engineering in Dental Sciences* (ed. A. Vishwakarma, P. Sharpe, S. Shi & M. Ramalingam), pp. 335-346. Boston: Academic Press.

Melendez, J., Liu, M., Sampson, L., Akunuru, S., Han, X., Vallance, J., Witte, D., Shroyer, N. and Zheng, Y. (2013). Cdc42 coordinates proliferation, polarity, migration, and differentiation of small intestinal epithelial cells in mice. *Gastroenterology* **145**, 808-819.

Mikels, A. J. and Nusse, R. (2006). Purified Wnt5a protein activates or inhibits beta-catenin-TCF signaling depending on receptor context. *PLoS Biol* **4**, e115-e115.

Minami, Y., Oishi, I., Endo, M. and Nishita, M. (2010). Ror-family receptor tyrosine kinases in noncanonical Wnt signaling: Their implications in developmental morphogenesis and human diseases. *Developmental Dynamics* **239**, 1-15.

Oishi, I., Suzuki, H., Onishi, N., Takada, R., Kani, S., Ohkawara, B., Koshida, I., Suzuki, K., Yamada, G., Schwabe, G. C., et al. (2003). The receptor tyrosine kinase Ror2 is involved in non-canonical Wnt5a/JNK signalling pathway. *Genes to Cells* **8**, 645-654.

Oka, S., Oka, K., Xu, X., Sasaki, T., Bringas, P., Jr. and Chai, Y. (2007). Cell autonomous requirement for TGF-beta signaling during odontoblast differentiation and dentin matrix formation. *Mechanisms of development* **124**, 409-415.

Oldridge, M., M Fortuna, A., Maringa, M., Propping, P., Mansour, S., Pollitt, C., DeChiara, T. M., Kimble, R. B., Valenzuela, D. M., Yancopoulos, G. D., et al. (2000). Dominant mutations in ROR2, encoding an orphan receptor tyrosine kinase, cause brachydactyly type B. *Nature Genetics* **24**, 275-278.

Olson, M., Ashworth, A. and Hall, A. (1995). An essential role for Rho, Rac, and Cdc42 GTPases in cell cycle progression through G1. Science 269: 1270-1272. *Science (New York, N.Y.)* **269**, 1270-1272.

Patel, S., Alam, A., Pant, R. and Chattopadhyay, S. (2019). Wnt Signaling and Its Significance Within the Tumor Microenvironment: Novel Therapeutic Insights. *Frontiers in Immunology* **10**, 2872.

Pearson, R. B. and Thomas, G. (1995). Regulation of p70s6k/p85s6k and its role in the cell cycle. *Prog. Cell Cycle Res.* **1**, 21-32.

Perl, A.-K. T., Wert, S. E., Nagy, A., Lobe, C. G. and Whitsett, J. A. (2002). Early restriction of peripheral and proximal cell lineages during formation of the lung. *Proceedings of the National Academy of Sciences* **99**, 10482.

Roarty, K., Pfefferle, A. D., Creighton, C. J., Perou, C. M. and Rosen, J. M. (2017). Ror2-mediated alternative Wnt signaling regulates cell fate and adhesion during mammary tumor progression. *Oncogene* **36**, 5958-5968.

Schambony, A. and Wedlich, D. (2007). Wnt-5A/Ror2 Regulate Expression of XPAPC through an Alternative Noncanonical Signaling Pathway. *Developmental cell* **12**, 779-792.

Schwabe, G. C., B., T., Suring, K., Brieske, N., Tucker, A. S., Sharpe, P. T., P.T., S., Minami, Y. and Mundlos, S. (2004). Ror2 knockout mouse as a model for the developmental pathology of autosomal recessive Robinow syndrome. *Developmental Dynamics* **229**, 400-410.

Sohn, W. J., Choi, M. A., Yamamoto, H., Lee, S., Lee, Y., Jung, J. K., Jin, M. U., An, C. H., Jung, H. S., Suh, J. Y., et al. (2014). Contribution of mesenchymal proliferation in tooth root morphogenesis. *Journal of dental research* **93**, 78-83.

Sonntag, R., Giebeler, N., Nevzorova, Y. A., Bangen, J.-M., Fahrenkamp, D., Lambertz, D., Haas, U., Hu, W., Gassler, N., Cubero, F. J., et al. (2018). Cyclin E1 and cyclin-dependent kinase 2 are critical for initiation, but not for progression of hepatocellular carcinoma. *Proceedings of the National Academy of Sciences* **115**, 9282.

Stricker, S., Rauschenberger, V. and Schambony, A. (2017). Chapter Four - ROR-Family Receptor Tyrosine Kinases. In *Current Topics in Developmental Biology* (ed. A. Jenny), pp. 105-142: Academic Press.

Sun, B., Ye, X., Lin, L., Shen, M. and Jiang, T. (2015). Up-regulation of ROR2 is associated with unfavorable prognosis and tumor progression in cervical cancer. *Int J Clin Exp Pathol* **8**, 856-861.

Szczawinska-Poplonyk, A., Ploski, R., Bernatowska, E. and Pac, M. (2020). A Novel CDC42 Mutation in an 11-Year Old Child Manifesting as Syndromic Immunodeficiency, Autoinflammation, Hemophagocytic Lymphohistiocytosis, and Malignancy: A Case Report. *Frontiers in Immunology* **11**.

Wang, Y., Cox, M. K., Coricor, G., MacDougall, M. and Serra, R. (2013). Inactivation of Tgfbr2 in Osterix-Cre expressing dental mesenchyme disrupts molar root formation. *Developmental biology* **382**, 27-37.

Xie, W., Chow L.T. Paterson, A. J., Chin, E. and Kudlow, J. E. (1999). Conditional expression of the ErbB2 oncogene elicits reversible hyperplasia in stratified epithelia and up-regulation of TGFalpha expression in transgenic mice. *Oncogene* **18**, 3593-3607.

Yamashiro, T., Zheng, L., Shitaku, Y., Saito, M., Tsubakimoto, T., Takada, K., Takano-Yamamoto, T. and Thesleff, I. (2007). Wnt10a regulates dentin sialophosphoprotein mRNA expression and possibly links odontoblast differentiation and tooth morphogenesis. *Differentiation* **75**, 452-462.

Yang, Z. H., H., B., Qin, L. z., Ti, X., Ti, X. Y., Lei, S. G., Zhao, Y. Q., Wiggins, L., Liu, Y., Feng, J. Q., et al. (2013). Cessation of epithelial Bmp signaling switches the differentiation of crown epithelia to the root lineage in a beta-catenin-dependent manner. *Molecular and Cellular Biology* **33**, 4731-4744.

Yasuda, S., Taniguchi, H., Oceguera-Yanez, F., Ando, Y., Watanabe, S., Monypenny, J. and Narumiya, S. (2006). An essential role of Cdc42-like GTPases in mitosis of HeLa cells. *FEBS Letters* **580**, 3375-3380.

Zhan, T., Rindtorff, N. and Boutros, M. (2016). Wnt signaling in cancer. *Oncogene* **36**, 1461.

Figures

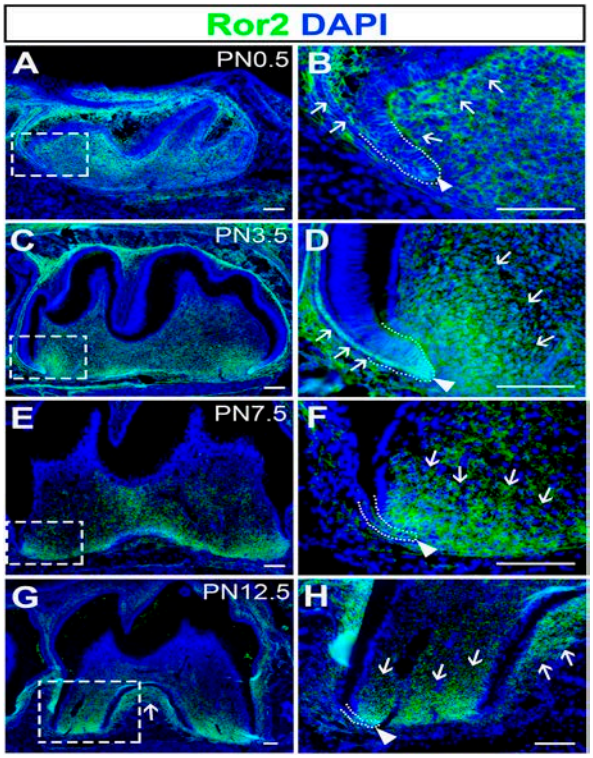

Figure 1. Ror2 is expressed in the dental mesenchyme and epithelium during tooth root development.

(A-H) Ror2 immunofluorescence of sagittal sections of mandibular molars from wild type mice at indicated stages from PN0.5 to PN12.5. Boxes in A, C, E and G are enlarged in B, D, F and H, respectively. Dotted lines indicate the border between dental epithelium and dental mesenchyme. Arrowheads indicate dental epithelium, and arrows indicate localization of Ror2 expression. Scale bars: 100μm.

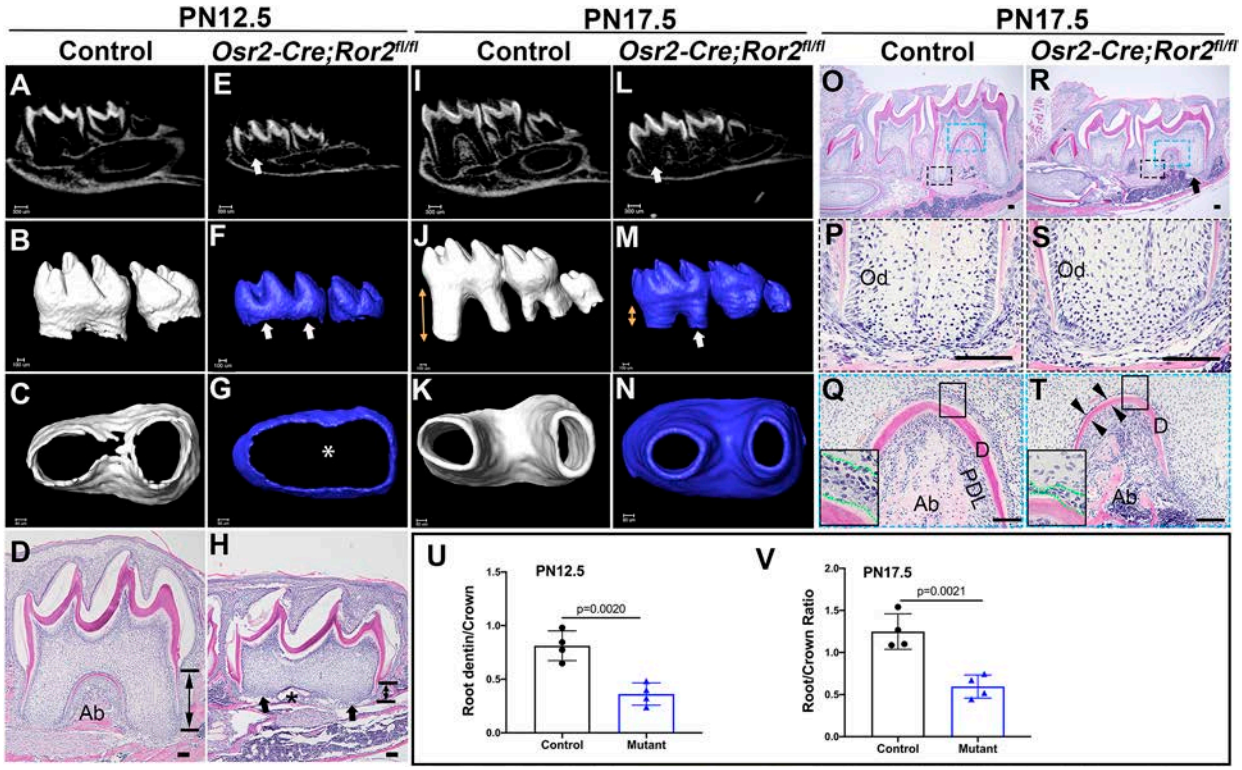

Figure 2. Loss of *Ror2* in the dental mesenchyme results in root development defects.

(A-H) MicroCT images and H&E staining of control (A-D) and *Osr2-Cre;Ror2* $^{fl/fl}$ (E-H) mandibular molars at PN12.5. Arrows indicate the apical region and asterisks indicate furcation region. Double-headed arrows in D and H indicate root dentin. AB=alveolar bone; N=4.

(I-N) MicroCT images of control (I-K) and *Osr2-Cre;Ror2* $^{fl/fl}$ (L-N) mandibular molars at PN17.5. Arrows indicate the apical region of the root and double-headed arrows indicate the length of the root. N=4.

(O-T) H&E staining of control (O-Q) and *Osr2-Cre;Ror2* $^{fl/fl}$ (R-T) mandibular molars at PN17.5. Boxes in O are enlarged in P and Q; boxes in R are enlarged in S and T. Arrows indicate the apical region of the root, and arrowheads indicate the dentin in the furcation region. Boxes in Q and T are shown in the insets at higher magnification to reveal the morphology of odontoblasts. Od=odontoblast; PDL=periodontal ligament; AB=alveolar bone; D=dentin. Scale bars: D, H, O-T, 100μm.

(U and V) Quantification analysis of the ratio of root to crown in control and *Osr2-Cre;Ror2* $^{fl/fl}$ (mutant) mice at PN12.5 and PN17.5 (N=4; Student's *t*-test).

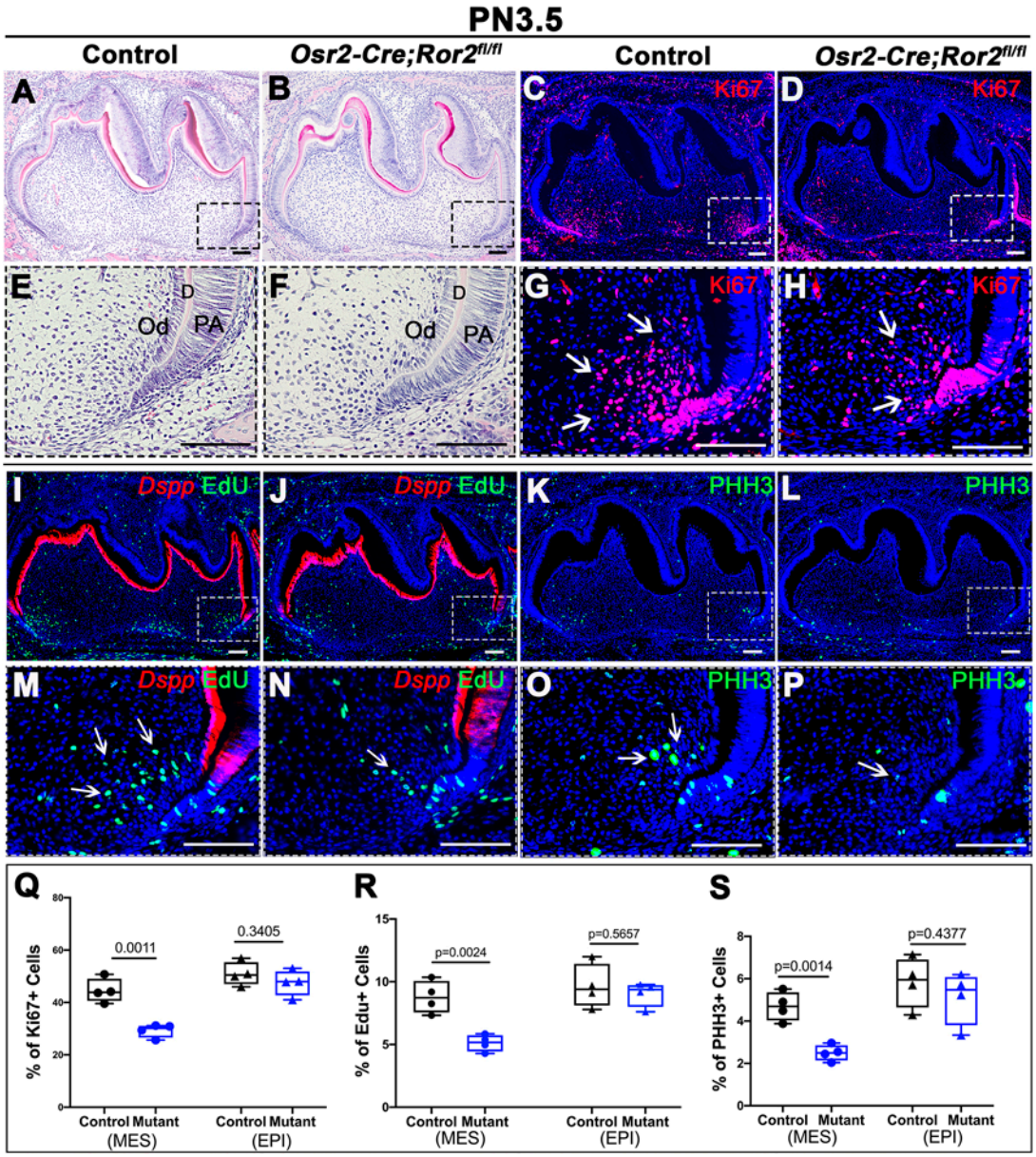

Figure 3. Loss of *Ror2* in dental mesenchyme decreases mesenchymal cell proliferation.

(A, B and E, F) H&E staining of control (A, E) and *Osr2-Cre;Ror2* $^{fl/fl}$ (B,F) mandibular molars at PN3.5. Boxes in A and B are enlarged in E and F, respectively. Od=odontoblast; D=dentin; PA=pre-ameloblast.

(C, D and G, H) Ki67 immunofluorescence (red) indicating proliferating cells in sagittal sections of mandibular molars in control (C, G) and *Osr2-Cre;Ror2* $^{fl/fl}$ (D, H) mandibular molars at PN3.5. Boxes in C and D are enlarged in G and H, respectively.

(I, J and M, N) RNAscope *in situ* hybridization of *Dspp* (red) and EdU assay (green) in control (I, M) and *Osr2-Cre;Ror2* $^{fl/fl}$ (J, N) mandibular molars at PN3.5 two hours after EdU injection. Boxes in I and J are enlarged in M and N, respectively. Arrows indicate positive signals.

(K, L and O, P) PHH3 immunofluorescence (green) indicating mitotic cells in control (K, O) and *Osr2-Cre;Ror2* $^{fl/fl}$ (L, P) mandibular molars at PN3.5. Boxes in K and L are enlarged in O and P, respectively. Arrows indicate positive signals. Scale bars:100 μm.

(Q-S) Quantification of Ki67-positive cells (Q), EdU-labeled cells (R) and PHH3-positive cells (S) in dental mesenchyme and dental epithelium in the apical region shown in G, H, M, N, O and P (N=4; Student's *t*-test). MES=mesenchyme; EPI=epithelium.

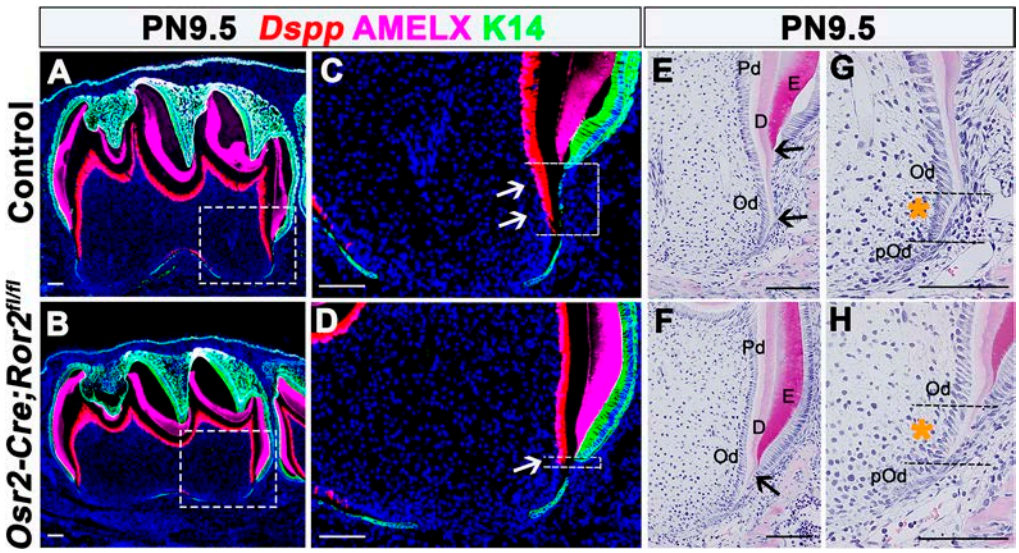

Figure 4. Loss of *Ror2* in dental mesenchyme disrupts differentiation of odontoblasts.

(A-D) RNAscope *in situ* hybridization of *Dspp* (red) and double immunostaining of Amelogenin X (AMELX, far red) and K14 (green) represent odonblasts, enamel and dental epithelium, respectively on sagittal sections of control (A, C) and *Osr2-Cre;Ror2* $^{fl/fl}$ (B, D) mandibular molars at PN9.5. Boxes in A and B are shown at higher magnification in C and D, respectively. Arrows and dotted lines in C, D indicate *Dspp*-positive cells below the enamel level.

(E-H) Histological analysis of dentin formation (E, F) and morphology of odontoblasts (G, H) in the apical region from control and *Osr2-Cre;Ror2* $^{fl/fl}$ mice. Arrows indicate root dentin. Yellow asterisks between dotted lines indicate the odontoblasts between differentiated odontoblasts and preodontoblasts. Od=odontoblast; pOd=preodontoblast; Pd=pre-dentin; D=dentin; E=enamel. Scale bars:100 μm.

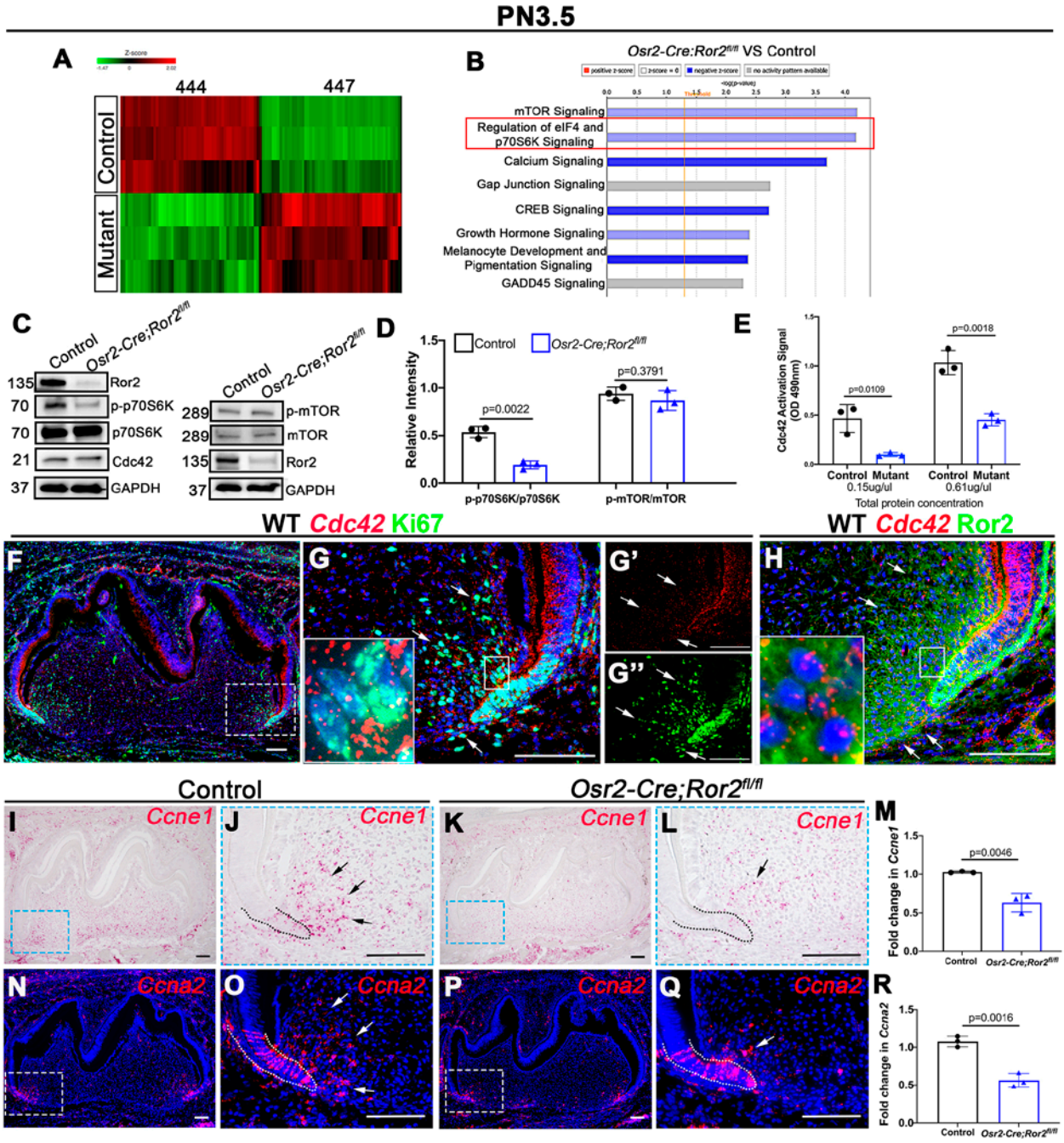

Figure 5. Putative downstream targets after loss of *Ror2* in dental mesenchyme.

(A) Heat map showing the gene expression profiles of dental mesenchyme in control and *Osr2-Cre;Ror2* $^{fl/fl}$ (mutant) mandibular molars at PN3.5.

(B) Ingenuity Pathway Analysis based on RNA-seq data shows the downregulation of eIF4 and p70S6K signaling in *Osr2-Cre;Ror2* $^{fl/fl}$ mice (indicated by the box).

(C)Western blot of Ror2, Cdc42, p70S6K, p-p70S6K, mTOR, p-mTOR and GAPDH in the dental mesenchyme from control and *Osr2-Cre;Ror2* $^{fl/fl}$ mice at PN3.5.

(D) Quantification of the relative intensity of p-p70S6K/p70S6K and p-mTOR/mTOR based on western blotting analysis (N=3; Student's *t*-test).

(E) The level of Cdc42 activation was measured in both equalized protein concentrations (0.15µg/µl and 0.61µg/µl) from control and *Osr2-Cre;Ror2* $^{fl/fl}$ (mutant) molars at PN3.5 by reading at OD490nm (N=3; Student's *t*-test).

(F, G) RNAscope *in situ* hybridization of *Cdc42* (red) and immunostaining of Ki67 (green) on sagittal sections of mandibular molars from wild type mice at PN3.5. The box in F is shown at higher magnification in G (merged), G'(*Cdc42*) and G'' (Ki67). The small box in G is shown in the inset at higher magnification to reveal the expression of *Cdc42* and Ki67 in the dental mesenchymal cells.

(H) RNAscope *in situ* hybridization of *Cdc42* (red) and immunostaining of Ror2 (green) on sagittal sections of mandibular molars from wild type mice at PN3.5. The small box in H is shown in the inset at higher magnification to reveal the expression of *Cdc42* and Ror2 in the dental mesenchymal cells.

(I-R) RNAscope *in situ* hybridization of *Ccne1* (I-M) and *Ccna2* (N-R) in control and *Osr2-Cre;Ror2* $^{fl/fl}$ mandibular molars at PN3.5 with quantification of their expression (M, R; N=3, Student's *t*-test). Boxes in I, K, N and P are shown at higher magnification in J, L, O and Q, respectively. Arrows indicate positive signals. Dotted lines indicate the border between dental epithelium and dental mesenchyme. Scale bars:100µm.

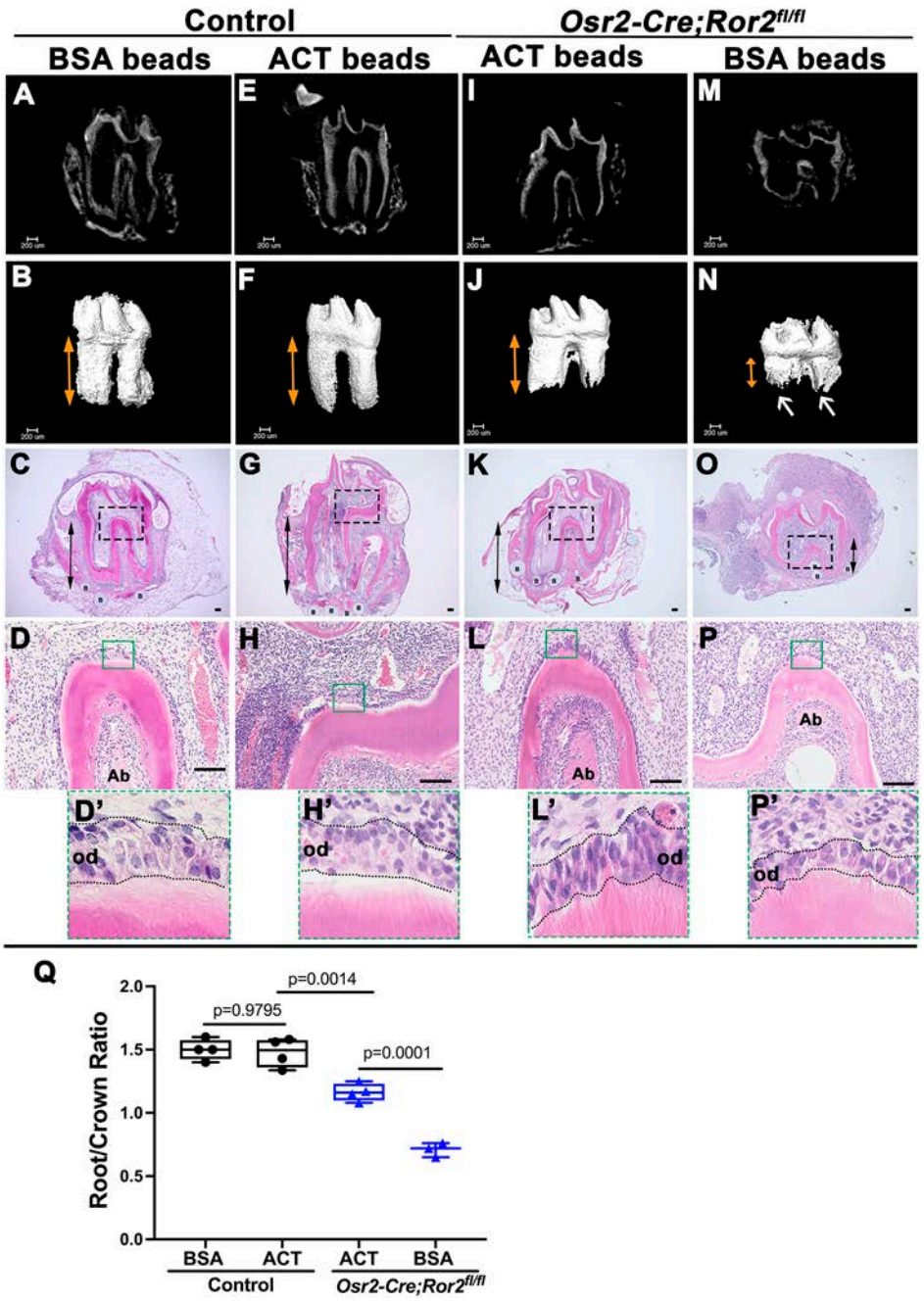

Figure 6. Cdc42 activator partially rescues root development in *Ror2* mutant mice.

(A-P) MicroCT images and H&E staining of control (A-H) and *Osr2-Cre;Ror2* $^{fl/fl}$ (I-P) mandibular molars after 3 weeks of cultivation under kidney capsules with BSA-soaked beads or activator-soaked beads since PN4.5. The control explants develop normal root length and root number (N=4; A-H). *Osr2-Cre;Ror2* $^{fl/fl}$ mandibular molars treated with Cdc42 activator-soaked beads show normal root formation (N=4; I-L) but are still shorter than the control molars (A-H). The *Ror2* mutant molars treated with BSA-soaked beads form a shorter root (N=3; M-P).

Double-headed arrows indicate tooth roots. Boxes in C, G, K and O are shown at higher magnification in D, H, L and P, respectively. Boxes in D, H, L and P show the morphology of odontoblasts (highlighted with dotted lines) in the furcation region at higher magnification in D', H', L' and P', respectively. Scale bars:100 μm.

(Q) Quantification of the ratio of root to crown in control molars and *Osr2-Cre;Ror2* $^{fl/fl}$ molars treated with BSA-soaked beads or activator-soaked beads (two-way ANOVA). B=beads; Od=odontoblast; Ab=alveolar bone; ACT=activator-soaked beads.

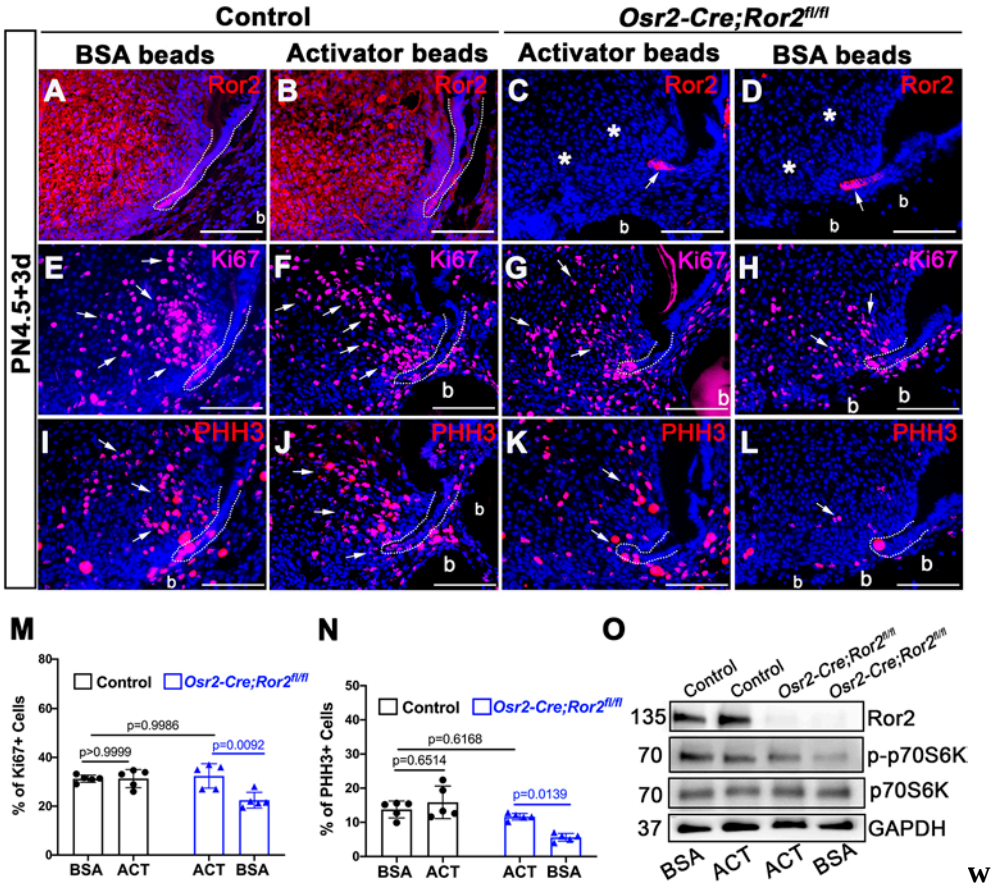

Figure 7. Cdc42 activator restores cell proliferation in *Ror2* mutant mice.

(A-D) Ror2 expression patterns in control (A, B) and *Osr2-Cre;Ror2* $^{fl/fl}$ (C, D) mandibular molars treated with BSA- or Cdc42 activator-soaked beads for 3 days in the kidney capsule since PN4.5. Dotted lines indicate the border between dental epithelium and dental mesenchyme. Asterisks indicate ablation of Ror2 in the dental mesenchyme. Arrows indicate the presence of Ror2 in dental epithelium.

(E-L) Ki67 immunofluorescence (E-H) indicating proliferating cells and PHH3 immunofluorescence (I-L) indicating mitotic cells in the apical region in sagittal sections of mandibular molars treated with BSA- or activator-soaked beads for 3 days in the kidney capsule since PN4.5. Dotted lines indicate the border between dental epithelium and dental mesenchyme. Arrows indicate positive signals. Scale bars:100 μm.

(M and N) Quantification of Ki67-positive cells (M) and PHH3-positive cells (N) in the apical region of control and *Osr2-Cre;Ror2* $^{fl/fl}$ molars treated with BSA- or activator-soaked beads for 3 days in the kidney capsule since PN4.5 (N=5; two-way ANOVA).

(O) Western blot of Ror2, p70S6K, p-p70S6K and GAPDH in the dental mesenchyme of control and *Osr2-Cre;Ror2* $^{fl/fl}$ molars treated with BSA- or activator-soaked beads for 2 days under kidney capsule since PN4.5. ACT=activator beads.

SUPPLEMENTARY INFORMATION

Supplementary Figures

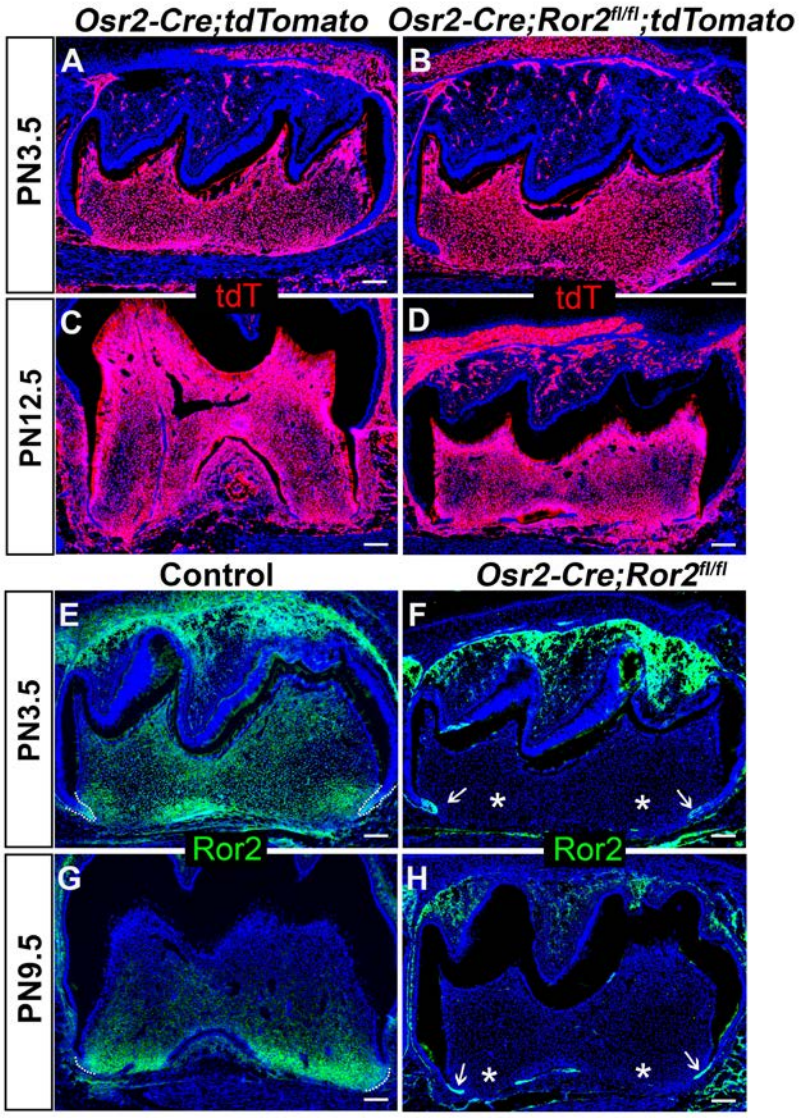

Figure S1. Ror2 is efficiently deleted in the dental mesenchyme in *Osr2-Cre;Ror2 $^{fl/fl}$* mice. (A-D) tdTomato immunostaining of sagittal sections of molars from *Osr2-Cre;tdTomato* and *Osr2-Cre;Ror2 $^{fl/fl}$;tdTomato* mice at PN3.5 (A, B) and PN12.5 (C, D). (E-H) Ror2 expression patterns in control and *Osr2-Cre;Ror2 $^{fl/fl}$* mandibular molars at PN3.5 (E, F) and PN9.5 (G, H). Asterisks indicate ablation of Ror2 in the dental mesenchyme. Arrows indicate the presence of Ror2 in dental epithelium. tdT=tdTomato. Scale bars:100 μm.

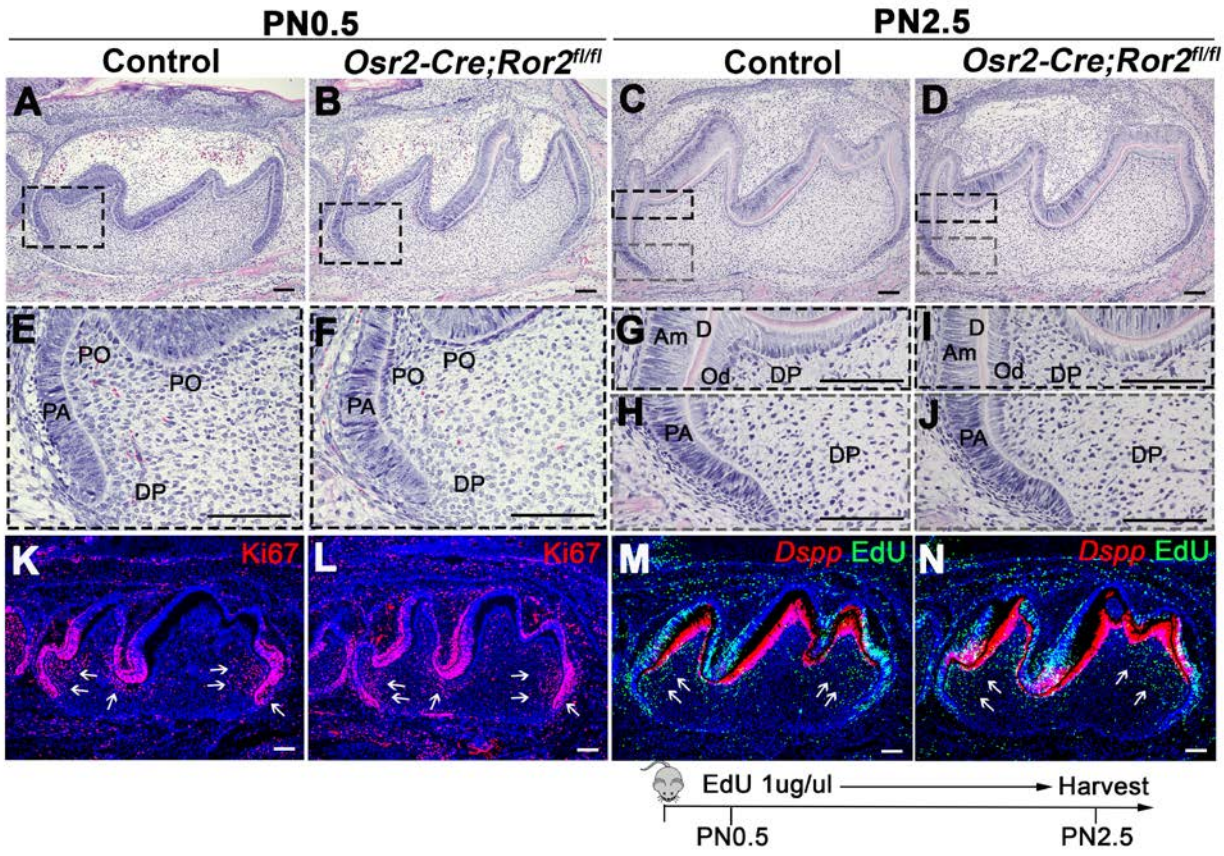

Figure S2. Loss of *Ror2* in the dental mesenchyme does not affect crown formation.
(A-J) Histological analysis of control and *Osr2-Cre;Ror2* $^{fl/fl}$ mandibular molars at PN0.5 (A, B, E, F) and PN2.5 (C, D, G, H, I, J). Boxes in A and B are enlarged in E and F, respectively. Boxes in C are enlarged in G and H, and boxes in D are enlarged in I and J. DP= dental pulp; PA=pre-ameloblast; PO=pre-odontoblast; Am=ameloblast; Od=odontoblast; D=dentin. (K, L) Ki67 immunofluorescence (red) indicating proliferating cells in sagittal sections of mandibular molars in control (K) and *Osr2-Cre;Ror2* $^{fl/fl}$ (L) mandibular molars at PN0.5. Arrows indicate positive signals. (M, N) RNAscope *in situ* hybridization of *Dspp* (red) and EdU assay (green) in control (M) and *Osr2-Cre;Ror2* $^{fl/fl}$ (N) mandibular molars at PN2.5, two days after EdU injection at PN0.5. Arrows indicate EdU positive signals. Schematic at the bottom indicates injection protocol. Scale bars:100 µm.

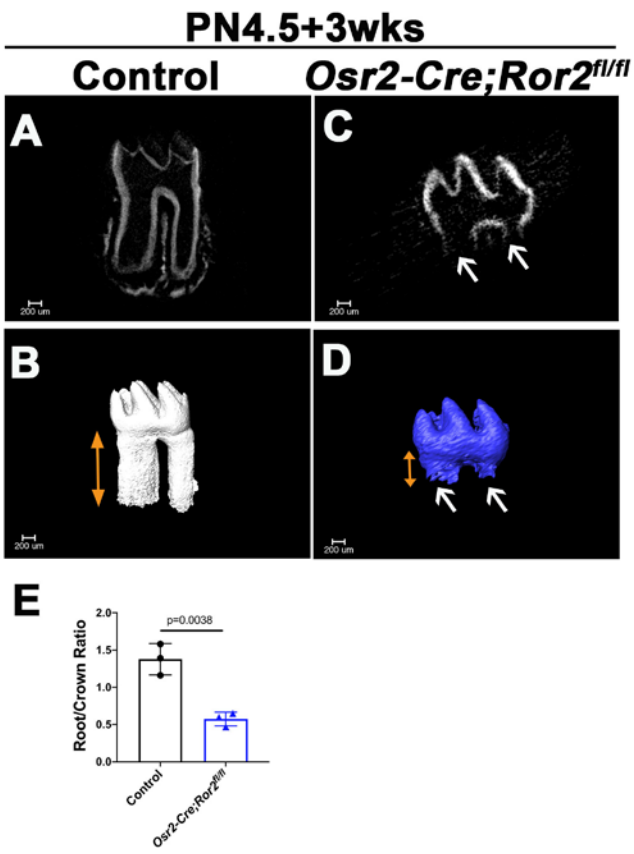

Figure S3. Loss of *Ror2* leads to shortened roots in *Osr2-Cre;Ror2* $^{fl/fl}$ molars in kidney capsule transplantation. MicroCT images of control (A, B) and *Osr2-Cre;Ror2* $^{fl/fl}$ (C, D) mandibular molars after 3 weeks of cultivation under kidney capsules since PN4.5. (E) Quantification of the ratio of root to crown in control molars and *Osr2-Cre;Ror2* $^{fl/fl}$ molars cultivated under kidney capsule. Arrows indicate the apical region of the roots and double-headed arrows indicate tooth roots.

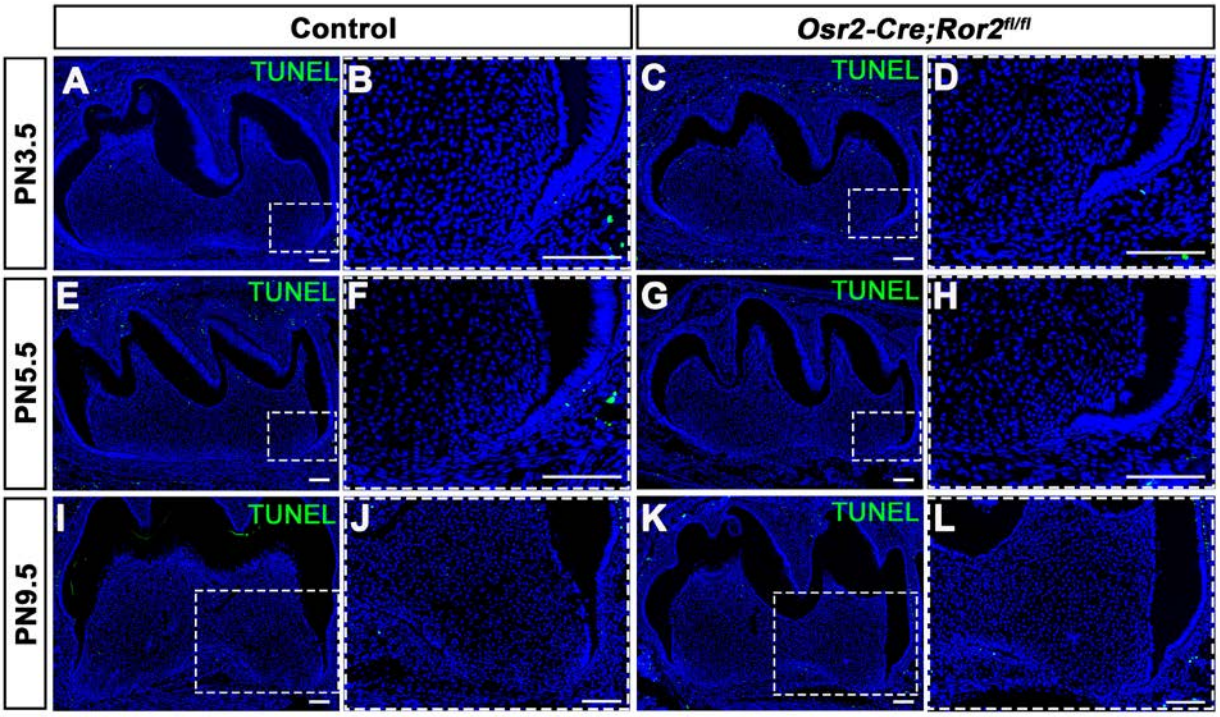

Figure S4. Cell apoptosis is unchanged in the apical region of *Osr2-Cre;Ror2 $^{fl/fl}$* mandibular molars. (A-L) TUNEL assay of sagittal sections of mandibular molars from control and *Osr2-Cre;Ror2 $^{fl/fl}$* mice at PN3.5 (A-D), PN5.5 (E-H) and PN9.5 (I-L). Boxes in A, C, E, G, I and K are enlarged in B, D, F, H, J and L, respectively. Scale bars:100 µm.

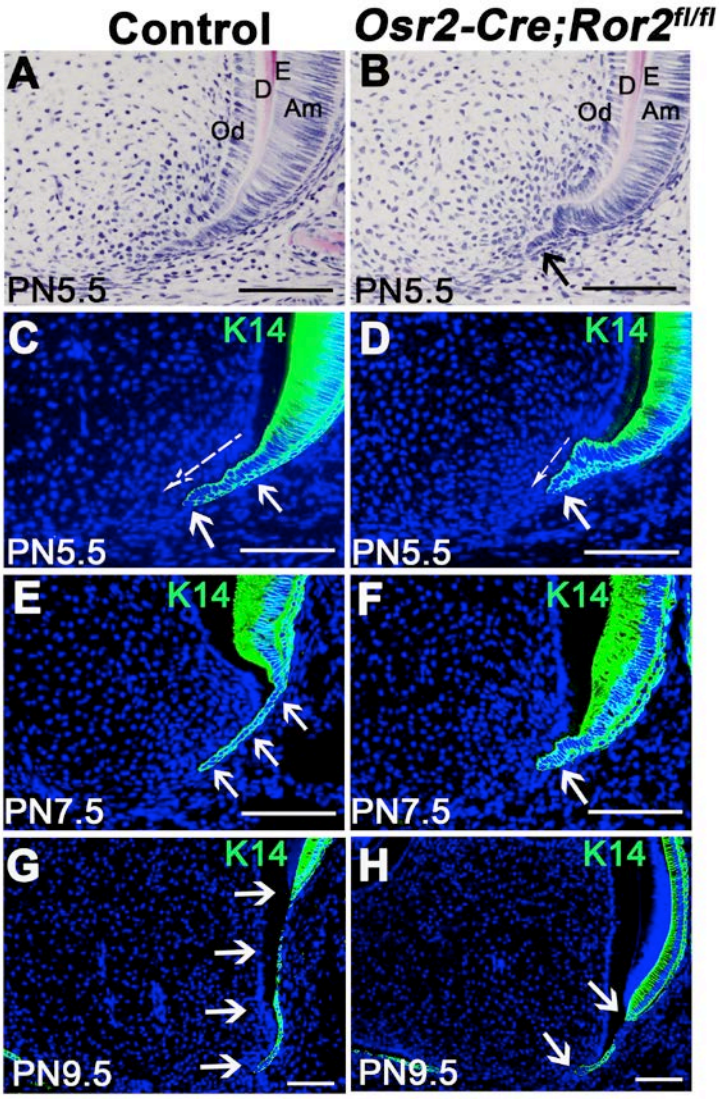

Figure S5. Epithelial diaphragm is compromised through tissue-tissue interaction after loss of *Ror2* in dental mesenchyme. (A, B) H&E staining of control (A) and *Osr2-Cre;Ror2* $^{fl/fl}$ (B) mandibular molars at PN5.5. Od=odontoblast; D=dentin; E=enamel; Am=ameloblast. Arrows indicate HERS. (C-H) K14 immunofluorescence (green) indicating the dental epithelium in sagittal sections of control and *Osr2-Cre;Ror2* $^{fl/fl}$ mandibular molars at PN5.5 (C, D), PN7.5 (E, F) and PN9.5 (G, H). Arrows indicate HERS. Scale bars:100 µm.

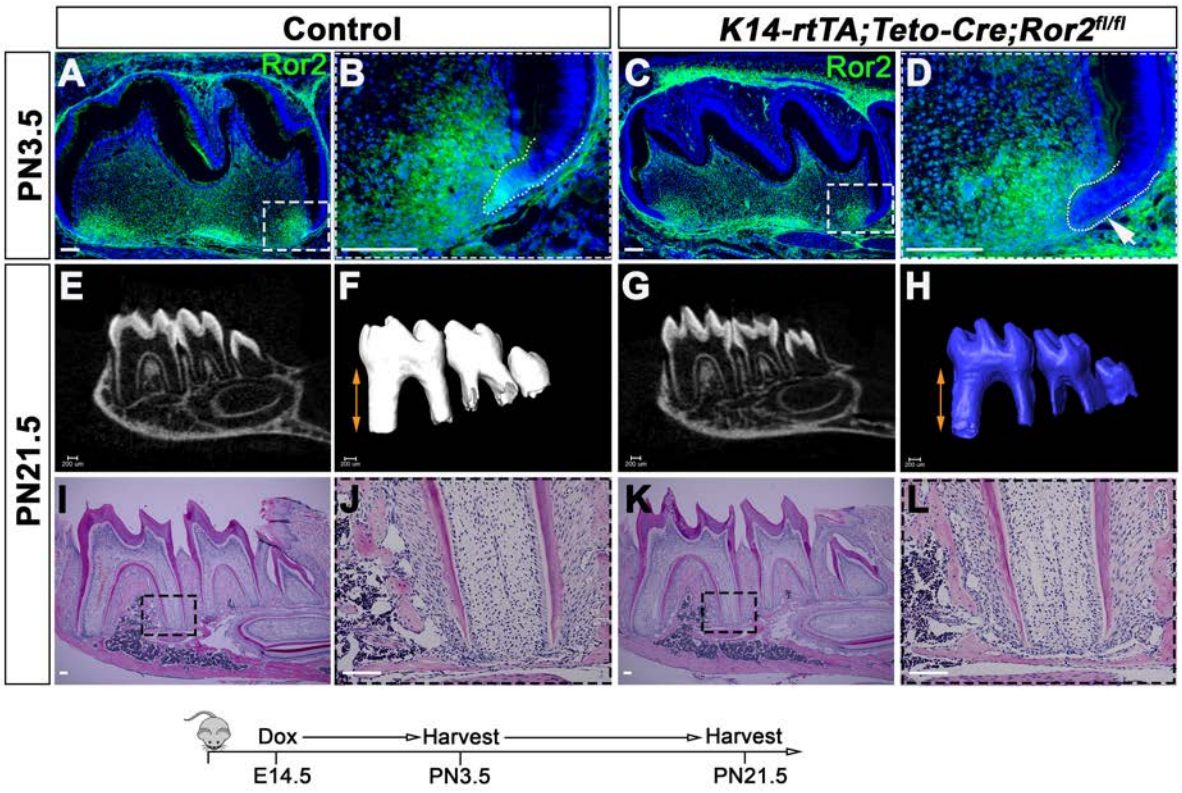

Figure S6. Loss of *Ror2* in the dental epithelium has no effect on root development.
(A-D) Ror2 is effectively deleted in the dental epithelium in *K14-rtTA;Teto-Cre;Ror2* $^{fl/fl}$ mice (C, D), compared to control mice (A, B) at PN3.5. Dotted lines indicate the border between dental epithelium and dental mesenchyme. The arrow indicates the lack of positive signal in the dental epithelium. Scale bars:100 µm. (E-H) MicroCT images of control (E, F) and *K14-rtTA;Teto-Cre;Ror2* $^{fl/fl}$ (G, H) mandibular molars at PN21.5. Double-headed arrows indicate tooth roots. (I-L) Histological analysis of control (I, J) and *K14-rtTA;Teto-Cre;Ror2* $^{fl/fl}$ (K, L) mandibular molars at PN21.5. Boxes in A, C, I and K are enlarged in B, D, J and L, respectively. Schematic at the bottom indicates induction protocol. Scale bars:100 µm.

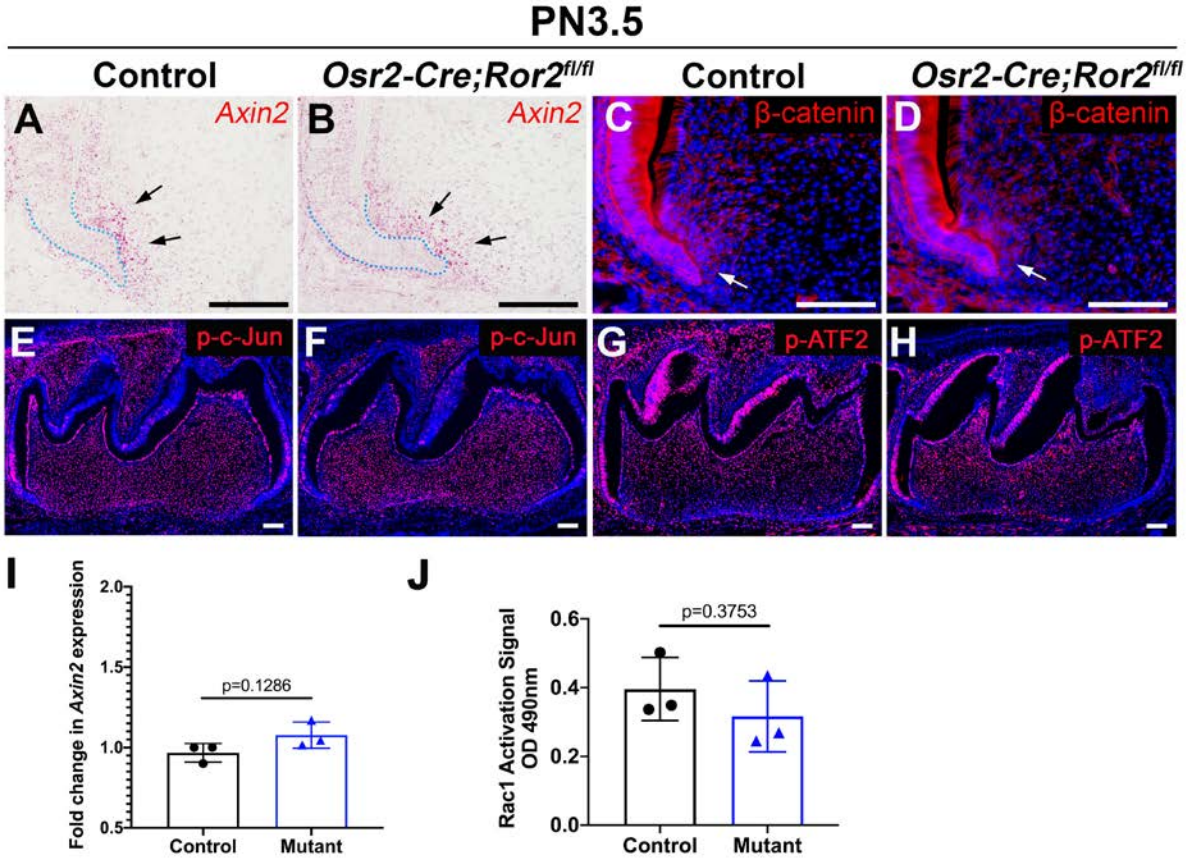

Figure S7. Canonical Wnt pathway and c-Jun/ATF2 activation are unaffected in *Osr2-Cre;Ror2 fl/fl* mandibular molars. (A-D**)** RNAscope *in situ* hybridization of *Axin2* (A, B) and immunostaining of active β-catenin (C, D) in the apical region of molars from control and *Osr2-Cre;Ror2 fl/fl* mice at PN3.5. Dotted lines indicate the border between dental epithelium and dental mesenchyme. Arrows indicate positive signals. (E-H) Phospho-c-Jun (p-c-Jun; E, F) and phospho-ATF2 (p-ATF2; G, H) immunostaining of sagittal sections of molars from control and *Osr2-Cre;Ror2 fl/fl* mice at PN3.5. (I) Fold change of *Axin2* expression in the dental mesenchyme from control and *Osr2-Cre;Ror2 fl/fl* (mutant) mandibular molars at PN3.5. Scale bars:100 µm. (J) The level of Rac1 activation was measured in tissue lysates from the dental mesenchyme in control and *Osr2-Cre;Ror2 fl/fl* (mutant) molars at PN3.5 by reading at OD490nm.

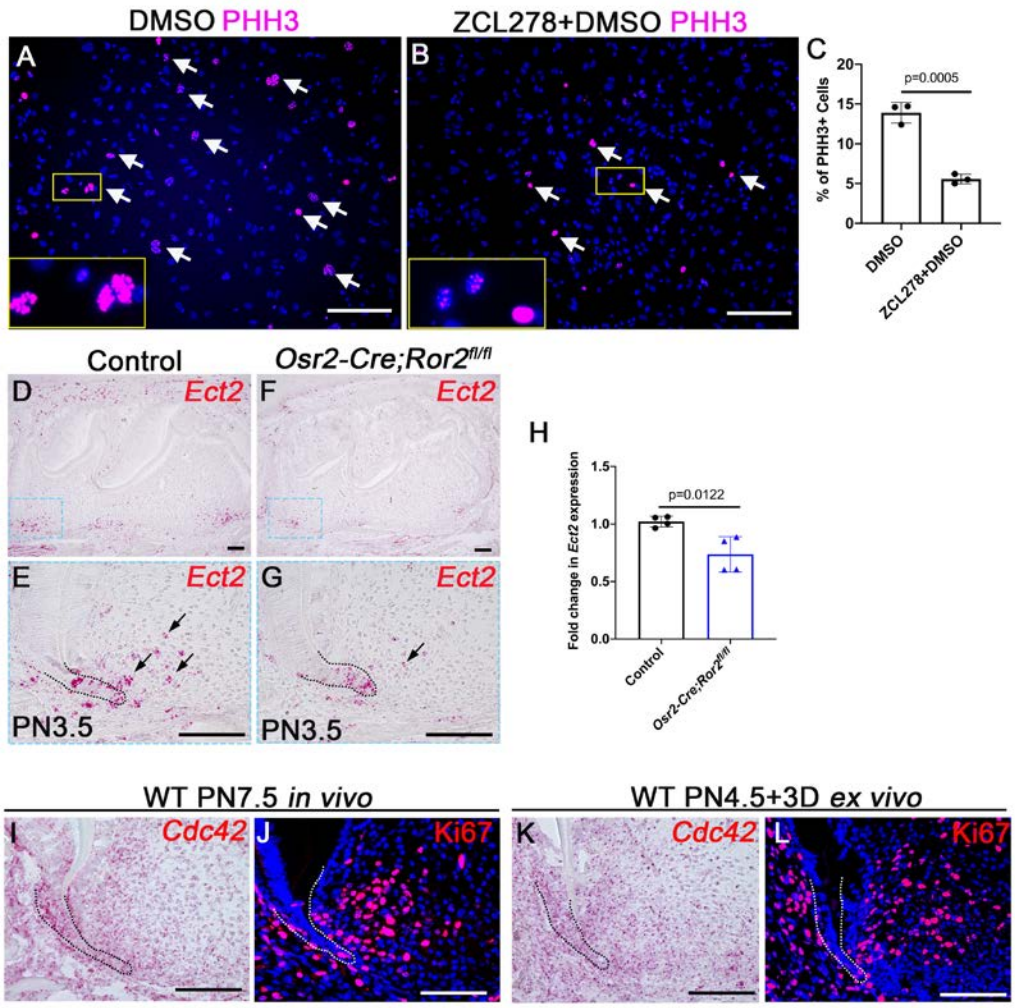

Figure S8. Putative downstream targets after loss of *Ror2* in dental mesenchyme.

(A-C) Immunofluorescence light microscopy of PHH3 in mesenchymal cells treated with DMSO (control; A) or Cdc42 inhibitor ZCL278 (B) and quantification of PHH3-positive cells (C). The small box in A/B is shown in the inset at higher magnification. Arrows indicate positive signals. (D-H) RNAscope *in situ* hybridization of *Ect2* in control (D, E) and *Osr2-Cre;Ror2* $^{fl/fl}$ (F, G) mandibular molars at PN3.5 with quantification of fold change in gene expression by qPCR (H; N=4, Student's *t*-test). Boxes in D and F are shown at higher magnification in E and G, respectively. Arrows indicate positive signals. (I-L) RNAscope *in situ* hybridization of *Cdc42* and immunostaining of Ki67 in wild type molars at PN7.5 *in vivo* (I, J) and after 3 days of cultivation under kidney capsule since PN4.5 (K, L). Dotted lines indicate the border between dental epithelium and dental mesenchyme.

Supplementary Tables

Table S1. List of PCR primers.

Gene	Forward sequence	Reverse sequence	Application
Gapdh	AGGTCGGTGTGAACGGATTTG	GGGGTCGTTGATGGCAACA	qRT-PCR
Ccne1	TGCACCAGTTTGCTTATGTT	CCGTGTCGTTGACATAGG	qRT-PCR
Ccna2	GGCTGACACTCTTTCCG	CTGGTAGCAAGAATTAGAGCAT	qRT-PCR
Axin2	AACCTATGCCCGTTTCCTCTA	GAGTGTAAAGACTTGGTCCACC	qRT-PCR
Ect2	AACTTGTGCTTGGCGTCTAC	CTCCCCTTTGTGCACAGTTG	qRT-PCR

Table S2. The 15 selected candidate genes generated from RNA-sequencing analysis

Gene Symbol	Gene Name	Total counts	Fold chang
Cnbd2	*Cyclic nucleotide-binding domain-containing protein 2*	2.73E+01	3.05
Ccne1	*Cyclin E1*	1.37E+01	-1.12
Ect2	*Epithelial cell transforming gene 2*	2.48E+01	-1.53
Ccnc	*Cyclin C*	7.08E+01	-1.61
Taf13	*Transcription initiation factor TF IID subunit 13*	8.17E+01	-1.65
Dock11	*Dedicator of cytokinesis protein 11*	5.61E+01	-1.71
Ccna2	*Cyclin A2*	6.84E+01	-1.74
Ccng1	*Cyclin G1*	3.67E+02	-1.75
Cbx3	*Chromobox Protein homolog 3*	4.70E+02	-1.94
Fgd3	*FYVE, RhoGEF and PH domain containing 3*	3.93E+01	-1.94
Vcan	*Versican*	2.34E+03	-2.01
Fgfr3	*Fibroblast growth factor receptor 3*	2.25E+02	-2.11
Rps6	*40S ribosomal protein S6*	2.56E+02	-2.21
Pdgfd	*Platelet-derived growth factor D*	1.53E+02	-2.51
Fgf13	*Fibroblast growth factor 13*	6.38E+01	-2.57

Table S3. All 891 differentially expressed genes generated from RNA-sequencing analysis

Click here to Download Table S1